

# The Sagittarius Dwarf Spheroidal Galaxy Survey (SDGS) II: The Stellar Content and Constraints on the Star Formation History.\*

M. Bellazzini,<sup>1</sup> F.R. Ferraro,<sup>1</sup> and R. Buonanno,<sup>2</sup>

<sup>1</sup>*Osservatorio Astronomico di Bologna, Via Ranzani 1, 40127 Bologna, ITALY*

<sup>2</sup>*Osservatorio Astronomico di Roma, Via dell'Osservatorio 2, 00040, Monte Porzio Catone, Roma, ITALY*

Accepted Received ; in original form

## ABSTRACT

A detailed study of the Star Formation History of the Sgr dSph galaxy is performed through the analysis of the data from the Sagittarius Dwarf Galaxy Survey (SDGS; Bellazzini, Ferraro & Buonanno 1999). Accurate statistical decontamination of the SDGS Color - Magnitude diagrams allow us to obtain many useful constraints on the age and metal content of the Sgr stellar populations in three different region of the galaxy.

A coarse metallicity distribution of Sgr stars is derived, ranging from  $[Fe/H] \sim -2.0$  to  $[Fe/H] \sim -0.7$ , the upper limit being somewhat higher in the central region of the galaxy. A qualitative global fit to all the observed CMD features is attempted, and a general scheme for the Star Formation History of the Sgr dSph is derived. According to this scheme, star formation began at very early time from a low metal content Inter Stellar Medium and lasted for several Gyr, coupled with progressive chemical enrichment. The Star Formation Rate (SFR) had a peak from 8 to 10 gyr ago when the mean metallicity was in the range  $-1.3 \leq [Fe/H] \leq -0.7$ . After that maximum, the SFR rapidly decreased and very low rate star formation took place until  $\sim 1 - 0.5$  Gyr ago.

**Key words:** Astronomical data bases; surveys; stars; photometry; Local Group galaxies.

## 1 INTRODUCTION

The recently discovered Sagittarius dwarf Spheroidal galaxy (Ibata et al. 1994; hereafter IGI-I) is the nearest satellite galaxy of the Milky Way. The structure of the Sgr dSph appears to be strongly disturbed by the interaction with the Galaxy and we are probably witnessing the ongoing process of merging of a dwarf galactic sub-unit into a main giant galaxy [see Ibata et al. 1995 (IGI-II); Ibata et al. 1997 (IWGIS); Mateo et al. 1995a (MUSKKK); Mateo et al. 1995b (MKSKKU); Mateo et al. 1996; Sarajedini & Layden 1995 (SL95); Marconi et al. 1998 (MAL), Whitelock, Irwin & Catchpole 1996 (WIC); Fahlman et al. 1998 (FAL); Montegriffo et al. 1998 (MoAL), for further discussions and references].

Thus Sgr represents a unique opportunity to study in detail the stellar content and the Star Formation History

(SFH) of a dwarf spheroidal galaxy, and the possible influence of the interactions with a parent galaxy on the SFH itself. Furthermore the study of the Sgr galaxy can be an ideal testbed for many relevant open problems in astrophysics, as, for instance, the comprehension of the evolutionary path of dwarf galaxies (Grebel 1998), the dark matter content of dSph's and the formation of the Milky Way halo and/or bulge (Johnston 1998, Fusi Pecci et al. 1995, Majewsky 1996).

However, the detailed analysis of the Sgr stellar content represent a hard observational challenge, because of (a) the very low surface brightness (i.e. number of stars per unit area) of the galaxy, and (b) the high degree of contamination by foreground stars belonging to the Milky Way Bulge and Disc.

In a companion paper (Bellazzini, Ferraro & Buonanno 1999; hereafter PAP-I) we presented the data and the first results of a large photometric survey, the Sagittarius Dwarf Galaxy Survey (SDGS), aimed to the study of the stellar

\* Based on data taken at the New Technology Telescope - ESO, La Silla.

content of the Sgr galaxy and specifically planned to attempt overcoming the problems (a) and (b) described above.

The scientific rationale of the SDGS is:

- To collect photometric data for a large number of stars in the direction of Sgr, in order to sample adequately the Post Main Sequence (PMS) branches in the Color - Magnitude Diagram (CMD) and providing the natural complement to the HST photometry by Mighell et al. (1997).
- To obtain a significant sample of the foreground population contaminating the Sgr fields, in order to attempt to disentangle the CMD features of the Sgr galaxy from those associated with the Galactic field.
- To observe different regions of the Sgr galaxy searching for possible spatial variations in the stellar content.
- To provide constraints on the age and metallicity of the Sgr stellar populations, trying to reconstruct the main events of the SFH.

The main characteristics of the SDGS and the results of PAP-I will be summarized in Sect. 2, in order to set the basis for the analysis performed in the present paper, in which we discuss the decontaminated CMDs and their main features.

In Sect. 3 the decontamination method is presented and tested. Sect. 4 is devoted to the detailed analysis of the decontaminated CMDs, and to a comparison between the stellar content of the different fields. Sect. 5 reports the results about the metallicity distribution of Sgr stars, and in Sect. 6 we report age estimates. A new general scheme for the Star Formation History in the Sgr galaxy is proposed. Discussion and conclusions are presented in Sect. 7.

## 2 NOMENCLATURE AND RESULTS OF PAP-I

In this section we briefly summarize the contents of PAP-I for an easier comprehension of the present paper.

### 2.1 Observed fields and completeness of the samples

Three wide fields ( $\sim 35 \times 9 \text{ arcmin}^2$ ) have been observed toward the Sgr galaxy:

- SGR12, located at  $(l; b) \sim (6; -14)$ , sampling the densest clump of the Sgr galaxy, near the M54 globular cluster (see IGI-II and IWGIS). Calibrated V and I magnitude has been obtained for a total of 25793 stars, with a typical limiting magnitude of  $V \sim 21.8$ . Because of bad weather conditions, for a considerable region of this field (nearly 2/5) we got acceptable photometry only down to  $V \sim 18.5$ . So the complete sample (SGR12) is used only when the analysis is limited to the bright part of the CMD, otherwise the best quality sample (SGR12R; 16992 stars) is adopted.
- SGR34, located at  $(l; b) \sim (6.5; -16)$ , sampling the second density clump of the galaxy (see IGI-II). A total of 22603 stars have been measured, with a typical limiting magnitude of  $V \sim 22.5$ .
- SGRWEST, located at  $(l; b) \sim (5; -12)$ , sampling a region near the edge of the Sgr galaxy (as seen in the IWGIS isodensity map) toward the Galactic Bulge. A total of 41462 stars have been measured, with a typical limiting magnitude of  $V \sim 22.5$ .

The above fields are nearly oriented along the Sgr major axis (IWGIS), SGR34 is  $\sim 2 \text{ deg}$  eastward from SGR12 and SGRWEST is  $\sim 2 \text{ deg}$  westward from SGR12.

A fourth control field of  $24 \times 9 \text{ arcmin}^2$  (GAL) has been observed in a region devoid of Sgr stars  $[(l; b) \sim (354; -14)]$ . The sample contains 8836 stars, with a limiting magnitude of  $V \sim 22$ .

The spatial distribution of stars in the SDGS fields is quite homogeneous and the crowding conditions are never critical. The completeness of the various samples is found to be very similar (see PAP-I).

### 2.2 Reddening and degree of foreground contamination

The interstellar extinction within each of the observed fields is rather homogeneous. The reddening in the SGR34 field was assumed  $E(V - I) = 0.22 \pm 0.04$ , as measured by MUSKKA (see PAP-I). Minor reddening differences were found between the SGR34 and the other SDGS fields, and the corresponding corrections have been applied to report all the samples at the same reddening of the reference field SGR34. The extinction relations by Rieke & Lebofski (1985; hereafter RL) has been always adopted both in PAP-I and in the present paper.

The various SDGS fields are affected by different amount of foreground star contamination, since there is a strong density gradient in the Galactic Bulge (and Disc, to a lesser extent) passing from  $b = -16^\circ$  to  $b = -12^\circ$ . The degree of contamination was estimated with respect to the GAL field. It turned out that the density of stars belonging to the contaminating population (CP) is nearly the same for the SGR34 and the GAL fields, while is  $\sim 1.6$  times higher in SGR12 and  $\sim 3.6$  times higher in SGRWEST (see Sect. 3.2 for an account of the limitations of this approach).

### 2.3 The two main stellar populations in Sgr

The inspection of a typical Sgr CMD (MUSKKA, MAL, PAP-I) reveals that the dominant stellar population is an intermediate-old one, with an extended RGB and a clumpy red Horizontal Branch (HB). Different authors (MUSKKA, FAL, MAL) agrees that this component is some Gyr younger than a typical globular cluster, the actual age (and age difference) depending on the assumed metallicity (see PAP-I and Sect. 6). In PAP-I we referred to this main population as Sgr Pop A. It is still unclear if Pop A is a *single age* population but it seems ascertained that a metallicity spread is present (see PAP-I and references therein).

MUSKKA and MAL showed that a clear sequence of blue stars is also present above the MS Turn Off (TO) of Pop A, in the region of the CMD that is often populated by Blue Stragglers (BS). Given the low stellar density in the Sgr galaxy and the detection of Carbon Stars (IGI-II, WIC) this sequence (hereafter Blue Plume) has been interpreted as an extended Main Sequence, signature of more recent star formation events. In PAP-I we named this younger population Pop B and we showed that its spatial distribution is similar to that of Pop A.

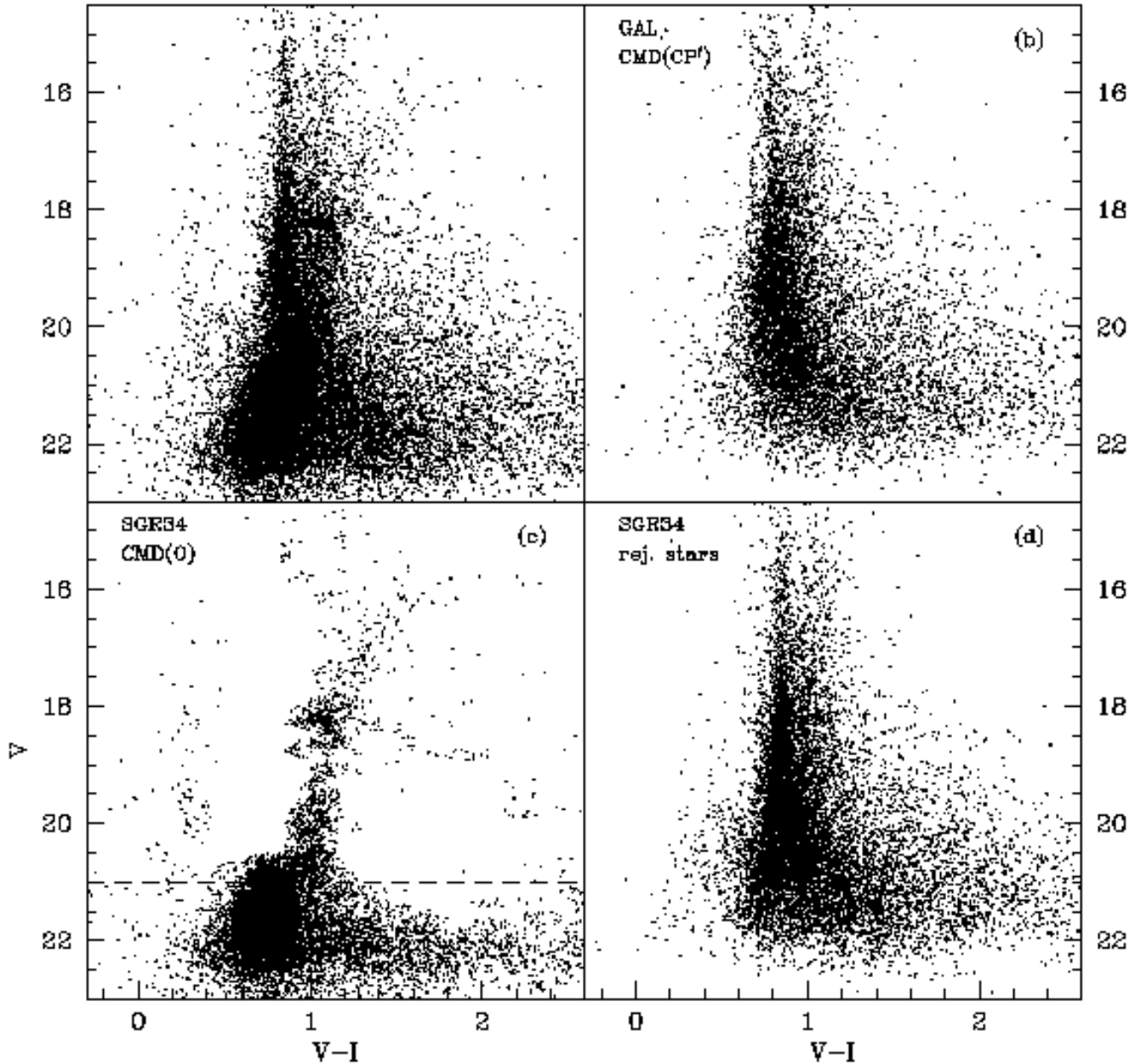


**Figure 1.** Decontamination of the SGR34 CMD(O+CP) [panel (a), 22559 stars] with the GAL CMD(CP) [panel (b), 8291 stars]. The decontaminated CMD(O) is shown in panel (c) (11036 stars) while the CMD of the stars rejected by the decontaminating algorithm, as putative CP members, is displayed in panel (d) (11523 stars).

#### 2.4 Analysis of non-decontaminated CMDs

As we will show below, while statistical decontamination is in principle the standard way to deal with strongly contaminated CMDs and has been successfully performed in many cases (see Mighell et al. 1996 - hereafter MRSF - for example), the actual application to the Sgr galaxy is very difficult. Up to now, the only attempt has been done by MUSKKE who provided a *smoothed and integrated* (see MUSKKE)

CMD of a ( $15 \times 15 \text{ arcmin}^2$ ) field at the same position of SGR34.

On the other hand, all authors (MUSKKE, SL95, IWGIS, MAL) tried to take advantage of the fact that many important features of the Sgr CMD [as for example the brightest part of the RGB or the red HB] emerges sufficiently clearly from the sequences produced by the contaminating foreground stars. Following this approach and comparing the Sgr CMDs to the GAL one we obtained a number of results

about distance, HB morphology etc. These results will be recalled below, when necessary.

The most interesting result of PAP-I was the detection of a very metal poor component of the Sgr galaxy (similar to Ter 8,  $[Fe/H] = -2.0$ ) that can be associated with a possible older population.

### 3 STATISTICAL DECONTAMINATION OF CMDs

The basic idea of the Statistical Decontamination (SD) of a CMD is very simple. We indicate with  $O$  (*Object*) the intrinsic population of the studied stellar system and with  $CP$  the contaminating population. The observed CMD [hereafter  $CMD(O + CP)$ ] shows the contribution of both the intrinsic and contaminating populations. The latter contribution to  $CMD(O + CP)$  can be estimated using a corresponding CMD of an adjacent field containing only foreground/background stars ( $CP'$ ), under the assumption that it is statistically representative of the contaminating population ( $CP' \sim CP$ ). The  $CP$  contribution on the  $CMD(O + CP)$  is removed by comparing the local density of stars in the two diagrams,  $CMD(O + CP)$  versus  $CMD(CP')$ :

$$CMD(O + CP) - CMD(CP') \sim CMD(O)$$

Obviously the technique can give optimal results when (a) the degree of field contamination is moderate, i.e. the  $CMD(O+CP)$  is not dominated by  $CP$ ; (b) the  $CP'$  sample is representative of the  $CP$  population either in type and in density (see PAP-I), and (c) the Object features on the CMD are intrinsically well defined and well populated, since a clear-cut local overdensity in  $CMD(O+CP)$  with respect to  $CMD(CP')$  is the fundamental key for a star to enter in the  $CMD(O)$  sample.

As it shall be shown below, requirement (a) is only marginally fulfilled by the SGR34 and SGR12 samples while a good decontamination for SGRWEST results impossible due to overwhelming foreground contamination (see Sect. 3.2 and 4.3).

In PAP-I we demonstrated that the GAL sample is fairly representative of the  $CP$  present in the SGR34 CMD. Furthermore we estimated the degree of contamination of the SGR12 and SGRWEST fields with respect to SGR34. In the following we perform SDs scaling the  $CP'$  local densities to the estimated degree of contamination.

Concerning point (c), the low stellar density and the intrinsic metallicity spread of Sgr conspire against the realization of a truly clean  $CMD(O)$ , at least in the less populated sequences. However, thanks to the wide SDGS samples, useful decontaminated CMDs have been obtained.

#### 3.1 The adopted algorithm

In this paper we adopt an algorithm very similar to that described by MRSF. Given a star belonging to  $CMD(O + CP)$  and with coordinates  $[V_* \pm \sigma_v; (V - I)_* \pm \sigma_{(V-I)}]$  the number of stars falling into the ellipse of axis  $[MAX(\sigma_v, 0.1); MAX(\sigma_{(V-I)}, 0.1)]$  around  $(V_*, V - I_*)$  on the original diagram ( $N_{O+CP}$ ) and on the “pure foreground”

diagram ( $N_{CP'}$ ) are computed. The actual dimension of the cell is an important parameter since if the cell is too small then only few stars fall into and the derived probability would be of little statistical significance. This occurrence is prevented by setting a fixed minimum dimension of the cell.

On the other hand, if the cell is too large the local number star density can be influenced by stars belonging to a feature physically distinct to the one to which the considered star belongs. The effect can become very destructive in the faint part of a CMD where  $\sigma_V$  and  $\sigma_{(V-I)}$  are larger. To minimize the problem we weighted each star present in the cell with an elliptical bi-dimensional Gauss distribution, according to its distance from the center of the cell, so that a star in the vicinity of  $(V_*, V - I_*)$  gives a greater contribution to  $N_{O+CP}$  or  $N_{CP'}$  with respect to a star which fall near the edge of the cell itself. Many test (either on SDGS CMDs or on CMD of globular clusters artificially contaminated) showed that much cleaner and *stable*  $CMD(O)$  are obtained with this kind of cell than with a crude rectangular one. While in the case of very well defined Object loci and low contamination the two approaches can give equivalent results, in more difficult cases (as the present ones) the “weighted cell” technique is clearly preferable.

According to MRSF, the probability  $P$  that a given star in the  $CMD(O+CP)$  is actually an Object member is defined as follow:

$$P = 1 - MIN\left(\frac{\alpha N_{CP'}}{N_{O+CP}}, 1.0\right) \quad (1)$$

where  $\alpha$  is the ratio of the area of the  $O+CP$  field to the area of the  $CP'$  field. Once  $P$  is calculated for a given star, it is compared with a randomly drawn number  $0 < P' < 1$  and if  $P' \leq P$  the star is accepted as an Object member, otherwise it is rejected and considered as a  $CP$  member (see MRSF for a more detailed description).

#### 3.2 Applications

In the following decontaminations of the CMDs the parameter  $\alpha$  has been set to the appropriate area ratio. Furthermore we used this parameter to account for the different density of the  $CP$  population in the different CMDs (SGR34, SGR12 and SGRWEST). This “CP density tuning” was obtained by increasing the  $\alpha$  ratio by a factor which accounts for the different  $CP$  density with respect to our  $CP'$  sample GAL, according to the estimates of PAP-I. Being  $\alpha$  the pure area ratio, let's call  $\alpha'$  the final parameter adopted. For each considered field we determined  $\alpha'$  as follows:

- For SGR34:  $\alpha' = 1.0 \times \alpha$
- For SGR12:  $\alpha' = 1.6 \times \alpha$
- For SGRWEST:  $\alpha' = 3.6 \times \alpha$

It is important to stress that this approach is based on the implicit assumption that the  $CP$  in the various SDGS fields differs only in density, which in general is not true. The “CP density tuning” factors were derived from the normalization of star counts in a narrow box of the CMD in which the foreground population is dominant (see PAP-I). Changes in the stellar mix (for example in the ratio between bulge and disk stars) cannot be accounted for, and may lead

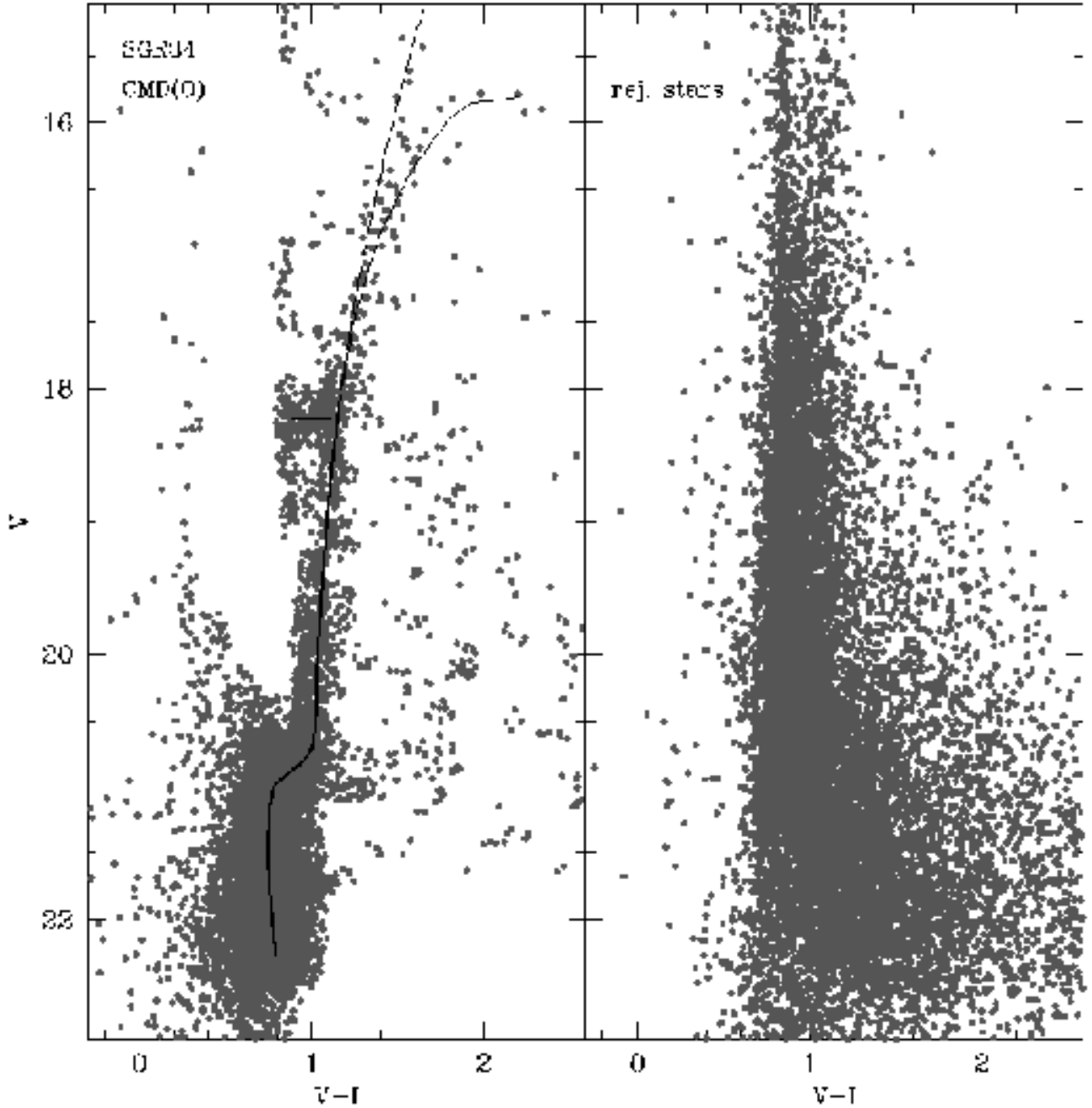


**Figure 2.** Decontamination of the SGR34 CMD(O+CP) [22559 stars] with the MCF CMD(CP) [13165 stars]. The decontaminated CMD(O) is shown in the left panel (9187 stars) while the CMD of the stars rejected by the decontaminating algorithm, as putative CP members, is displayed in the right panel (13372 stars). The faint parts of the decontaminated CMD presented here are clearly cleaner with respect to the CMD shown in the panel (c) of Fig. 1. The Pop A ridge line (see tab. 1) is superimposed to the CMD. Two different ridge lines are adopted for  $V < 18$  to account for the observed spread of the RGB stars.

to the adoption of density tuning factors which are not adequate for other regions of the CMD. Some of the results presented in this paper may be affected by this additional uncertainty (in particular those presented in Sect. 5.1).

The rationale of the adopted decontamination strategy has been widely discussed in PAP-I, together with *pros* and

*cons* of possible alternative approaches. Suffice to say here that the present application is optimized to recover the Sgr features on the CMD that are more vexed by foreground contamination, i.e. the upper MS, the SGB and the lower RGB (see Fig. 1).

**Table 1.** SGR34 Pop A - Ridge line.

V	V-I for $V \geq 18$	V-I RGB <i>red</i>	V-I RGB <i>blue</i>	V HB	V-I HB
15.14	-	-	1.645	-	-
15.5	-	-	1.569	-	-
15.80	-	2.202	-	-	-
15.82	-	2.104	-	-	-
15.89	-	1.880	-	-	-
16	-	1.783	1.463	-	-
16.5	-	1.521	1.376	-	-
17	-	1.354	1.298	-	-
17.5	-	1.247	1.23	-	-
18	1.176	1.176	1.176	18.23	0.876
18.5	1.126	-	-	18.23	1.116
19	1.088	-	-	-	-
19.5	1.06	-	-	-	-
20.05	1.034	-	-	-	-
20.55	1.017	-	-	-	-
20.75	0.980	-	-	-	-
20.8	0.955	-	-	-	-
20.85	0.908	-	-	-	-
20.9	0.860	-	-	-	-
20.95	0.810	-	-	-	-
21	0.780	-	-	-	-
21.16	0.753	-	-	-	-
21.26	0.751	-	-	-	-
21.43	0.749	-	-	-	-
21.50	0.744	-	-	-	-
21.57	0.751	-	-	-	-
21.67	0.756	-	-	-	-
21.89	0.764	-	-	-	-
22.28	0.794	-	-	-	-

In Fig. 1 the result of the decontamination of the SGR34 CMD using GAL as  $CP_I$  is shown. Panel (a) reports the original CMD(O+CP), panel (b) the CMD( $CP_I$ ) - i.e. the GAL CMD -, in panel (c) the decontaminated CMD(O) is presented and, finally, the CMD of the stars rejected by the subtraction algorithm (as putative CP members) is reported in panel (d). The horizontal line in panel (c) shows the level above which a reliable correction for completeness can be performed.

It results clear from Fig. 1 that the SD was largely successful. The *globular cluster -like* shape of Sgr Pop A clearly emerges in panel (c), the upper MS and the Sub Giant Branch (SGB) are now clear, while they were mostly obscured by CP stars in the original CMD. On the contrary, much of the residual contamination below  $V \sim 20.5$  is probably due to the relatively low limiting magnitude of the GAL sample (see PAP-I).

The effect of SD on the local density of stars in the various features of the final CMDs is hard to evaluate, also in the region of the CMD where completeness corrections can be performed. So, a detailed Luminosity Function could be affected by artificial bumps and gaps on small scales. Star counts remain a useful investigation tool when specific tests are applied (as those of PAP-I), i.e. counting stars in relatively large boxes around well populated features. On the other hand the SDs make available in a much clearer form the informations contained in the *shape* and *position* of the various CMDs features, i.e. - mainly - informations about age and metallicity.

In PAP-I it was suggested that the deeper CMD of the MUSKKE Control Field (hereafter MCF) can be used for decontamination of the SDGS diagrams, since the position of the field is the same of GAL. Few experiments showed that a superior decontamination of the faint part of CMDs can be obtained using MCF instead of GAL. In the following analysis MCF is adopted as the standard decontamination sample. The CMD shown in Fig. 1 (and the other obtained for SGR12 and SGRWEST using the GAL control field<sup>†</sup>) will be used as independent check of possible spurious features in the obtained CMD(O) due to small inhomogeneities between the SDGS and the MUSKKE control field samples. In Fig. 2 the results of the decontamination of the SGR34 CMD with the MCF CMD are presented [left panel: CMD(O); right panel: CMD of the rejected stars].

There are features common to all the decontaminated CMDs presented in this paper that deserve some comments. First, all the stars fainter than  $V \sim 17$  and redder than  $(V - I) \sim 1.2$  are obviously not members of Sgr, being mere residuals of the decontamination. Second, any apparent structure along the RGB (like gaps or small horizontal clumps) has to be considered as an artifact of the decontamination process.

#### 4 STATISTICALLY DECONTAMINATED CMDs: COMPARISONS BETWEEN SDGS FIELDS

Since SGR34 is the SDGS field which couples good photometric quality and the lowest degree of foreground contamination we first discuss the CMD(O) obtained from this field and then we will analyze the SGR12 and SGRWEST samples by comparison with SGR34. We will concentrate on the “globular cluster like” bulk of the Sgr population (Pop A). Pop B will be discussed in Sect. 6.4.

##### 4.1 The SGR34 field

The decontaminated CMD of the SGR34 field is very similar, in shape, to that of a typical (metal rich) globular cluster, with a faint TO region, an extended RGB and a stubby red HB around  $V \sim 18$ .

The average ridge line of the decontaminated SGR34 CMD (Pop A) is also presented in the left panel of Fig. 3 and in table 1. The line has been obtained by calculating the mean color in bins encompassing 0.1 mag from  $V = 22$  to  $V = 20.5$  and 0.5 mag from  $V = 20.5$  to  $V = 18$ , and then applying a  $2\text{-}\sigma$  clipping algorithm similar to that described by Sarajedini & Norris (1994). The spread of the stars in the brightest part of the RGB is such that an *average* ridge line would have little sense. We provide two different ridge lines for  $V < 18$ , representing the conservative range of RGB stars distribution in this portion of the CMD. In table 1 the two ridge lines adopted for  $V < 18$  are reported as RGB *blue* and RGB *red* according to their relative position in the CMD. Despite the large spread of the RGB, the Upper MS + SGB sequences are relatively narrow, very similar to those of a genuine globular cluster observed with the same

<sup>†</sup> Not shown here for obvious reasons of space

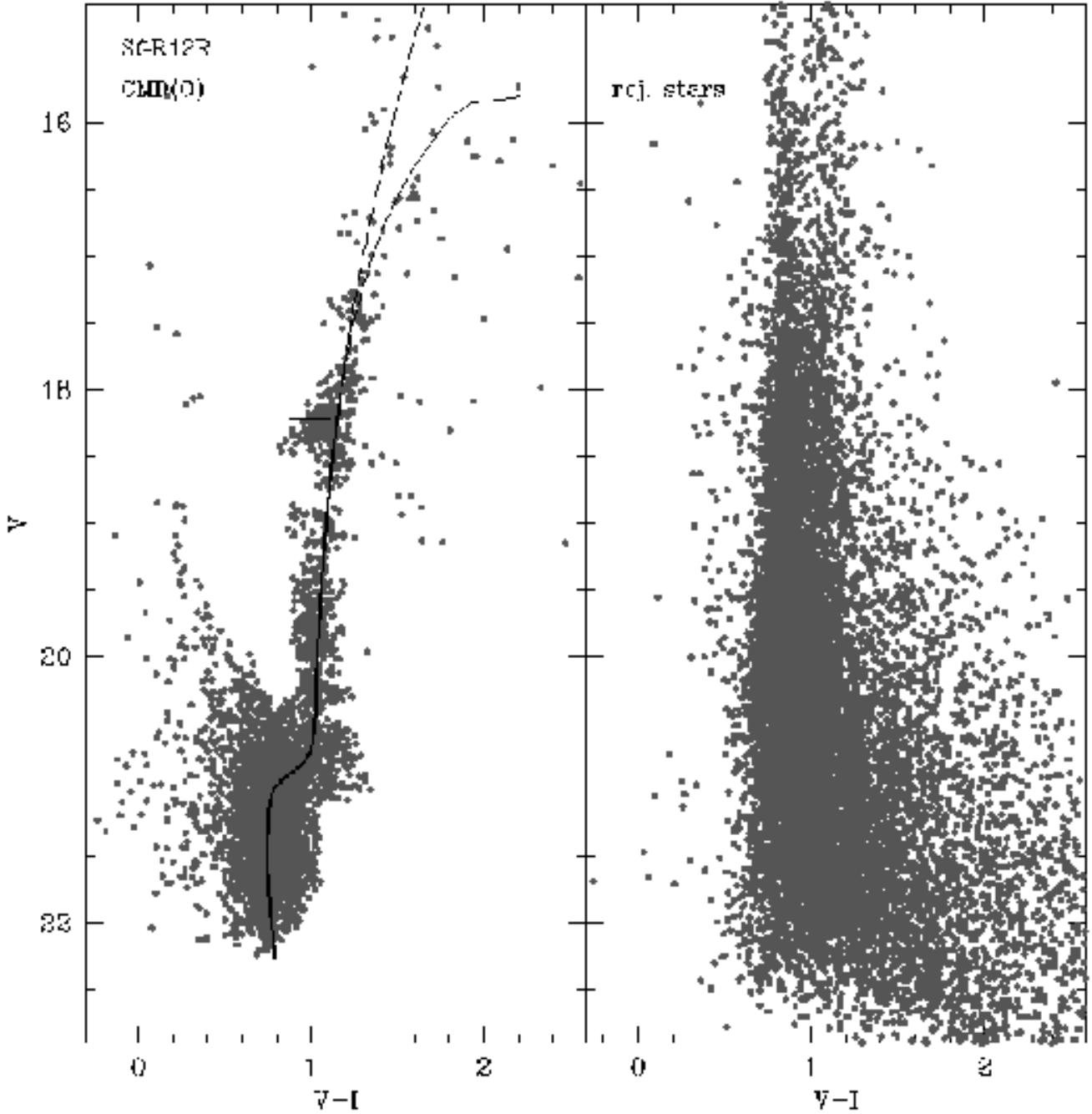


**Figure 3.** The same as Fig. 2 for the SGR12R sample (left panel: 4017 stars, right panel: 12936; total number of stars in the original CMD: 16953). The SGR34 ridge line has been superposed to allow a comparison between the main features of the CMDs in the two fields. The ridge line provides an excellent fit to the data (particularly in the TO region).

photometric precision (see the CMD of Ter 8 by MoAL, for instance). The “thin” SGB is particularly outstanding considering the photometric errors involved and the effects of the decontamination process.

Many “artificial decontamination” tests convinced us that the net effect of the decontamination process on a typical SGB is to widen it and that only *very sparse* sequences can be accidentally removed from the CMD by the cleaning

process. So, we are forced to conclude that the large majority of Pop A stars *share the same SGB sequence* within the photometric errors. This statement can have far reaching consequences, as we discuss in Sect. 6.

Sparse groups of stars appears nearly vertically aligned around  $(V - I) \sim 0.9$ , from  $V \sim 19$  to  $V \sim 15$ . This feature is not present in the analogous CMD(0) obtained using GAL

as  $CP'$  (see Fig. 1c) and consequently have to be considered as a spurious residual of the actual decontamination process.

On the other hand the presence of the above quoted Blue Plume and its association with the Sgr dSph has been robustly assessed in PAP-I, so it is no surprise to find it clearly emerging around [ $V \sim 20.5$ ;  $(V - I) \sim 0.4$ ]. Also this feature has an obvious counterpart in many galactic globulars as the well know BS sequence (see Ferraro, Fusi Pecci & Bellazzini 1995 and Bailyn 1995, for references), which is observed also in clusters of very low stellar density (e.g. NGC 5053, Nemeč & Cohen 1989). The main reason to associate the Sgr Blue Plume with the upper Main Sequence of a younger population (Pop B) is the detection of Carbon Stars (IWGIS, Whitelock, Irwin & Catchpole 1996; see also PAP-I) which unequivocally points to the presence of younger stars in the galaxy (e.g. Da Costa 1998). However it cannot be firmly established, at present, if all the Blue Plume stars are progenitors of the observed Carbon Stars or if a (perhaps significant) fraction of them is constituted by genuine BS stars.

If the Blue Plume is indeed an extended MS one would expect to observe also some SGB star associated with it, between the red edge of the Blue Plume itself and the base of the RGB of Pop A, while none is observed. Here we are facing the opposite situation with respect to the Pop A SGB (see above): Pop B SGB stars would be so few and so sparsely distributed in the CMD that would provide no significant local overdensity over the CP in this region, and probably have all been “erased” by the decontamination process. This fact would strongly lower our capability to constrain the SFH of Pop B (see Sect. 6.2).

#### 4.2 The SGR12 field

The decontaminated CMD of the SGR12R sample is shown in Fig.3 (left panel) together with the CMD of the rejected stars (right panel). The SGR34 ridge line already presented in Fig. 2 is superimposed to the decontaminated diagram to allow a direct comparison between the main Pop A features in the two fields.

The similarity is indeed remarkable, and the SGR34 ridge line fits very well all the observed SGR12R features. The only noticeable difference is the presence of stars significantly redder than the SGR34 ridge lines near the RGB tip, and the apparent redder HB morphology in the SGR12R sample with respect to the SGR34 one. Both differences have been already noted in PAP-I and tentatively interpreted as indications of the presence of more metal rich stars in the region of the Sgr galaxy covered by the SGR12 field (i.e., the center of density; see also SL95 and MAL). The difference in the distribution of RGB stars will be analyzed in detail in Sect. 5. Here we briefly discuss the difference in HB morphology.

Since the HB of the decontaminated SGR34 sample shown in Fig. 2 merges at the blue end with the spurious vertical sequence described in the previous section, we compare the HB morphology of the SGR34 and the SGR12R samples decontaminated with our own Control Field (GAL), including completeness corrections (see PAP-I).

In the upper panel of Fig. 4 the  $V - I$  histogram (normalized to the total number of stars) of the stars having  $17.5 < V < 18.5$  and  $0.55 < V - I < 1.2$  (see PAP-I) are

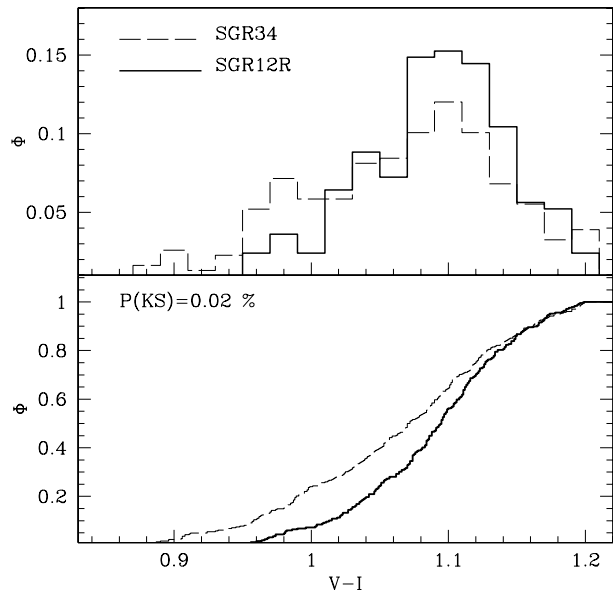


**Figure 4.** Upper panel:  $V - I$  color histograms (normalized to the total number of stars) of the HB stars for the SGR12R (bold continuous line) and the SGR34 (thin dashed line) samples. Lower panel: the cumulative distribution for the same stars. The probability that the two samples are extracted from the same parent population (according to a Kolmogorov-Smirnov test) is also reported on the upper left corner of the diagram.

reported for the SGR34 sample (thin dashed line) and for the SGR12R sample (bold continuous line). While the two distributions peak at the same color bin, the fraction of stars redder than  $V - I = 1.0$  is significantly higher for SGR12R, as can be readily appreciated from the cumulative distribution shown in the lower panel of Fig. 4. A Kolmogorov-Smirnov test (a test particularly well suited to analyze *shifts* between distributions) shows that the probability that the two samples are extracted from the same parent population is only 0.02%.

The analysis of the decontaminated CMD confirms the results of PAP-I: the HB morphology of the main population in the SGR12 field is slightly redder than in SGR34. It is important to stress that the present conclusion concerns the red part of the Sgr HB. To have a complete view of the morphology one have to take into account also RR Lyrae stars, which are certainly present (Mateo et al. 1995b, Alard 1996, Alcock et al. 1997), and blue HB stars, whose possible presence have been suggested in PAP-I.

#### 4.3 The SGRWEST field

As remarked in Sect. 3, the success of a statistical decontamination strongly depends on the relative surface density of CP and Object stars present in the observed field. The usual applications of the SD technique consists in the removal of a minority of field stars from the CMD of a populous cluster (see , for example, MRSF and Olsen et al. 1998).

From the performed decontaminations it results that

even in the less contaminated SDGS fields the majority of stars belong to the foreground population: 41% of stars are accepted as Sgr members in the SGR34 field and only 24% in the SGR12R one.

Since, as shown in PAP-I, the surface density of CP stars grows significantly toward low galactic latitudes, it is not surprising that a satisfying decontamination cannot be obtained for the SGRWEST CMD. The solution obtained following the prescriptions of Sect. 3 fails to remove all of the CP main sequence from the CMD, while it removes part of the Sgr RGB instead. The final decontaminated CMD can't allow further analysis and simply confirm the results obtained in PAP-I from the non-decontaminated CMD, i.e. (a) Sgr stars are present in the SGRWEST field, and (b) the overall CMD morphology is very similar to that observed in the other SDGS fields.

## 5 METALLICITY

In PAP-I we presented a preliminary comparison of the observed RGBs with the ridge lines of template galactic globulars from DCA90. Now we can perform a more detailed analysis on the decontaminated CMDs, using ridge lines derived from more recent photometry and covering the CMDs of the template clusters from the RGB tip to - at least - one magnitude below the MSTO. This will allow us to derive metallicity and age estimates with *the same* templates, with a fully consistent procedure.

The adopted ridge lines are taken from the following templates:

(i) M68 ( $[Fe/H] = -2.1$ ) from Walker (1994). The distance modulus was derived adopting his value of  $\langle V(RRLyrae) \rangle$  and applying the  $M_V(RRLyrae)$  vs.  $[Fe/H]$  relation by DCA90. From his estimate of the interstellar extinction  $E(V - I) = 0.09$  has been obtained and finally  $\mu_0 = 14.95$  has been adopted.

(ii) M3=NGC6752 ( $[Fe/H] = -1.34$ ) from Ferraro et al. 1997 adopting their estimates  $\mu_0 = 15.05$  and  $E(V - I) = 0.0$ . The ridge line of the MS+SGB in the  $(V; V-I)$  plane was not published by Ferraro et al. 1997 and has been derived directly from their data and joined with their RGB ridge line.

(iii) 47 Tuc=NGC104 ( $[Fe/H] = -0.71$ ) derived from the photometry of Kaluzny et al. (1998) adopting  $\mu_0 = 13.51$  and  $E(V - I) = 0.064$  according to DCA90. The photometry of Kaluzny does not cover the brightest part of the RGB. However the ridge line of DCA90 smoothly joints the one described above at  $M_V \sim 1.1$  and provides the ideal complement for the bright RGB.

(iv) NGC6528 ( $[Fe/H] = -0.35$ ) derived from the data of Ortolani et al. (1995). Adopting  $\mu_0 = 14.45$  and  $E(V - I) = 0.68$ , according to Bruzual et al. (1997), a significant mismatch is noted between the position of the HBs of SGR34 and NGC6528. A fair match is obtained if  $E(V - I) = 0.83$  is assumed, in good agreement with the alternative value proposed as by Bruzual et al. (1995),  $E(V - I) = 0.81$  (see their Note 2).

A further template will be used in Sect. 6, for the age analysis:

(v) Pal 1 ( $[Fe/H] = -0.7$ ) from Rosenberg et al. (1998a

hereafter R98; see also Rosenberg et al. 1998b for the spectroscopical metallicity measurement), adopting their  $E(V - I) = 0.20$ . R98 derived  $\mu_0 = 15.25 \pm 0.25$  by comparison with the ridge line of 47 Tuc by Hesser et al. (1987) and adopting  $\mu_0 = 13.35$  for this latter cluster. Since here we have always adopted  $\mu_0 = 13.51$  for 47 Tuc (also in deriving the distance modulus of Sgr, see PAP-I) we properly scaled the R98 distance modulus, obtaining  $\mu_0 = 15.41 \pm 0.25$  for Pal 1. In this way we set a fully (internally) consistent distance scale for Sgr, Pal 1 and 47 Tuc. The adoption of any alternative distance modulus for 47 Tuc would imply a corresponding correction in the moduli of Pal 1 and Sgr and the relative position of the ridge lines on the CMD would be unaffected.

The ridge line of Pal 1 is defined only up to the HB level. However the cluster has the same metallicity of 47 Tuc and the DCA90 ridge line for this cluster (represented in the plots as a dashed line) matches the line by R98 (continuous line) around  $M_V = 0.75$ , with the quoted distance and reddening assumptions, so it is adopted as the bright complement to the Pal 1 ridge line.

In Fig. 5, the bright part of the decontaminated CMD of SGR34 (left panel) and SGR12 (right panel) are reported in the absolute plane ( $M_V; (V - I)_0$ ) by adopting  $\mu_0 = 17.25$ ,  $E(V - I) = 0.22^\ddagger$ . The ridge lines of M68, M3, 47 Tuc and NGC 6528 are superimposed on the CMDs and the corresponding  $[Fe/H]$  values are marked near the ridge lines tips. The left panel of Fig. 5 shows that the bulk of the SGR34 RGB stars is nicely bracketed between the ridge lines of M3 and 47 Tuc. The distribution appears skewed toward the M3 ridge line and Sgr "putative member" stars bluer than this line are also present. No evident discontinuity in the distribution of stars between the quoted ridge lines is evident.

Interpreting the spread of the upper RGB as a spread in metal content between Sgr stars, we have that the majority of Sgr stars have  $-1.3 \leq [Fe/H] \leq -0.7$ , but the metallicity distribution probably reach a metallicity as low as  $[Fe/H] = -2.1$  (as shown also in PAP-I). Note that the global spread induced by photometric errors at the considered magnitude level is negligible (see PAP-I), so we are observing a physical spread in color.

The region of the CMD immediately below the almost vertical extension of the 47 Tuc ridge line ( $1.5 < (V - I)_0 < 2.3$  and  $M_V > -1.6$ ) is remarkably devoid of stars. This fact suggests  $[Fe/H] = -0.7$  as a firm upper limit to Sgr metallicity in this region of the galaxy. At  $M_V \sim -0.7$  and  $1.2 < (V - I)_0 < 1.8$  there are a few stars clustered around the ridge line of NGC6528 that could be tentatively associated with a sparse and very metal rich population. Most probably, they are spurious residuals of the decontamination as the stars with the same colors at  $M_V > 0$ .

The SGR12 case (Fig. 5, right panel) is very similar to the SGR34 one. The only apparent difference stands in the significant number of stars redder than the 47 Tuc ridge line, around  $M_V = -1.5$ . The metallicity spread of stars in this

<sup>‡</sup> It has to be recalled that differential reddening (and extinction) correction has already been applied to the SGR12 and SGRWEST samples to report them at the same reddening than SGR34 (see Sect. 2.2 and PAP-I). So the total correction to report the former two samples into the  $(M_V, (V - I)_0)$  plane are  $E(V - I) = 0.23$  for SGR12, and  $E(V - I) = 0.25$  for SGRWEST.

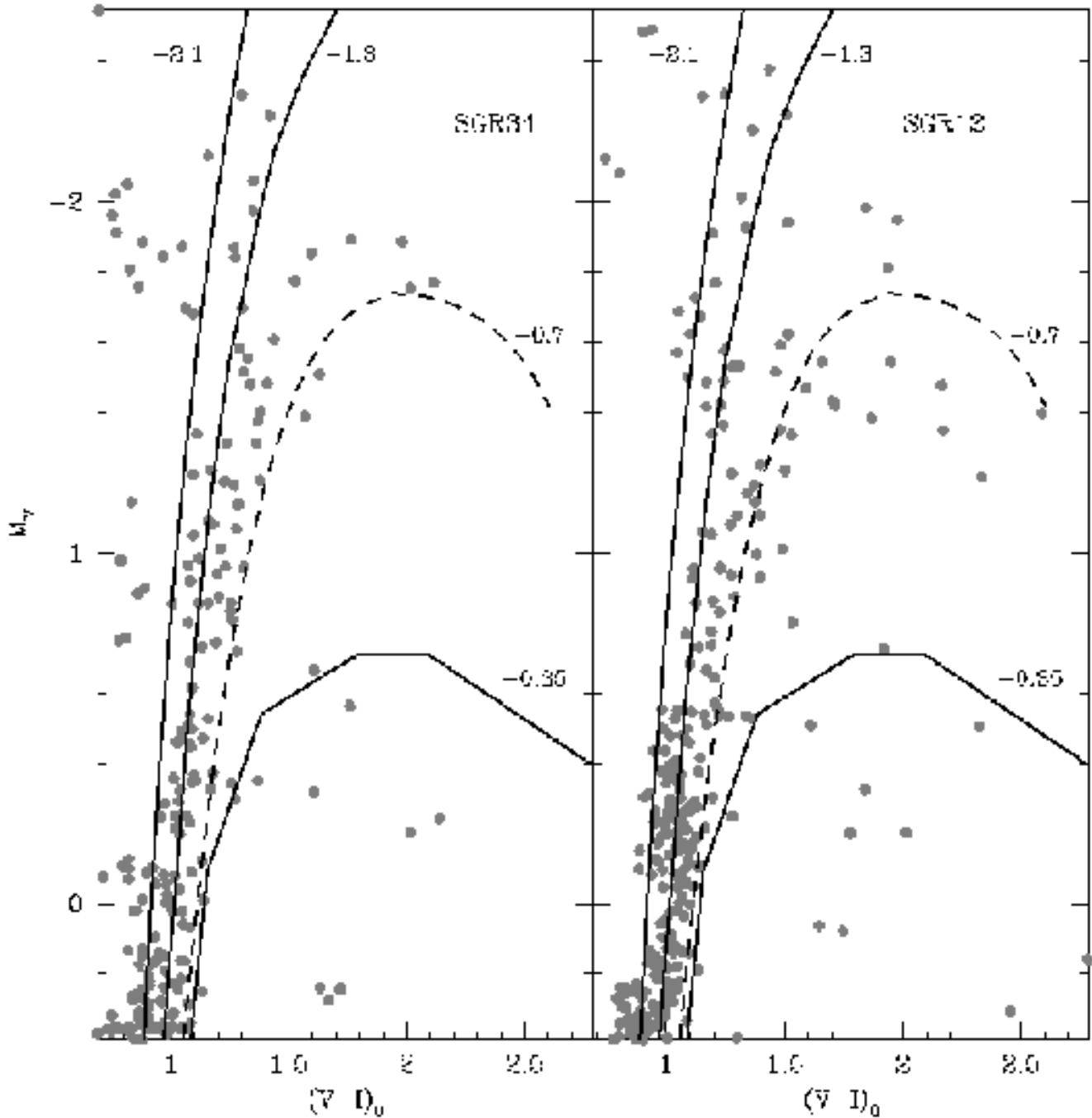


**Figure 5.** The bright part of the decontaminated CMD of SGR34 (left panel), and SGR12 (right panel) reported in the absolute plane. The superposed lines are the ridge lines of M68 ( $[Fe/H] = -2.1$ ), M3 ( $[Fe/H] = -1.34$ ), 47 Tuc ( $[Fe/H] = -0.71$ ), and NGC6528 ( $[Fe/H] = -0.35$ ), from left to right. The labels near the tip of the lines are the quoted  $[Fe/H]$  values.

field seems larger, with respect to SGR34, and the upper limit metallicity somewhat higher than  $[Fe/H] = -0.7$ , but still  $[Fe/H] < -0.35$ .

Evidences for a significant metallicity spread in Sgr Pop A has been already pointed out by many authors (MUSKKA, SL95, MAL) and appears to be confirmed by very recent high resolution spectroscopy of few Sgr giants

by Smecker-Hane et al. (1998), who find  $-1.5 \leq [Fe/H] \leq +0.11$  (see Sect. 4.3 and also Pasquini et al. 1999).

### 5.1 Metallicity distribution

Since a significant metallicity spread is evident in all the observed fields, it would be of paramount importance to

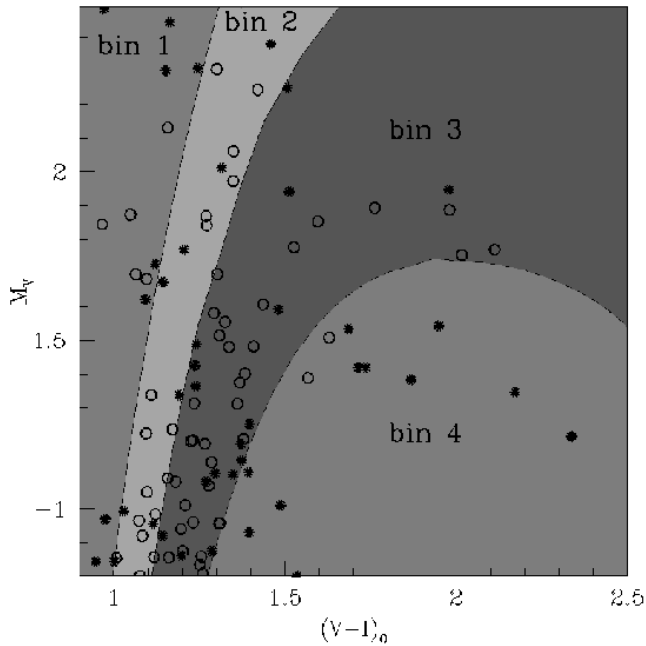


**Figure 6.** Metallicity bins used to derive the metallicity distribution displayed in Fig. 7. The ridge lines are the same of Fig. 5. Bin 1 corresponds to  $[Fe/H] < -2.1$ , bin 2 to  $-2.1 \leq [Fe/H] < -1.3$ , bin 3 to  $-1.3 \leq [Fe/H] < -0.7$ , and bin 4 to  $[Fe/H] \geq -0.7$ . Open circles are from the SGR34 sample, asterisks from the SGR12 sample.

know the **metallicity distribution** of Pop A stars. It is obvious that the right procedure to obtain such a distribution would imply accurate spectroscopic analysis that would lead simultaneously to a selection of *true member stars* and to a metallicity estimate of *each single measured star*. However this kind of project implies a huge observational effort, since to collect a statistically significant sample ( $\sim 50$ ) of Sgr members in just one of the SDGD fields, some 80-100 individual spectra have to be obtained (see Sect. 4.3). On the other hand the SDGS provides a total of more than 150 upper RGB stars ( $\sim 50$  per field) suitable for some photometric metallicity estimate. Their membership cannot be stated on a star by star basis but the *statistical membership* of the sample is robustly stated, since the upper part of the RGB is not seriously contaminated.

We obtained a coarse metallicity distribution of stars in each of the SDGS fields by the following steps:

- Only the portion of the CMDs of Fig. 5 delimited by  $(V-I)_0 > 0.9$  and  $-2.5 < M_V < -0.8$  has been considered, in order to avoid contamination of the sample by red HB stars or spurious residuals by the decontamination processes at very blue colors or too faint magnitudes.
- We counted the number of stars (1) bluer than the M68 ridge line, (2) lying between the M68 and the M3 ridge lines, (3) lying between the M3 and the 47 Tuc ridge lines, and (4) redder than the 47 Tuc ridge line. The described bins are illustrated in Fig. 6.
- The above defined bins were interpreted as coarse metallicity bins, according to the metallicity of the templates and in Fig. 7 we report the resulting histograms (upper

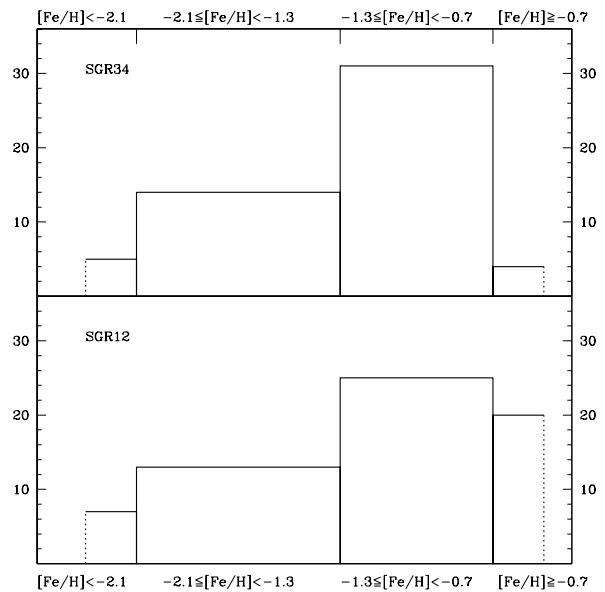


**Figure 7.** Coarse metallicity distributions in the SDGS fields from the distribution of stars in the upper RGB region of the CMDs.

panel: SGR34, lower panel: SGR12). The bin 1 and 4 have been devised to detect the limits of the metallicity distribution: a significant decrease of frequency in this bins strongly indicates respectively  $[Fe/H] = -2.1$  and  $[Fe/H] = -0.7$  as the true limits of the distribution. The left side of bin 1 and the right side of bin 4 histograms have been represented with dotted lines to indicate that, if a significant number of stars is indeed present in these bins a well defined metallicity limit cannot be assumed.

The two histograms are rather similar. The lower metallicity limit appear to be  $[Fe/H] = -2.1$  in both samples, confirming the results of PAP-I. The peak of the distribution is clearly in bin 3. The number of stars between  $-1.3 \leq [Fe/H] < -0.7$  is double than that in the  $-2.1 \leq [Fe/H] < -1.3$  bin. According to Fig. 7 it can be concluded that the Sgr galaxy produced more than 65% of Pop A stars at metallicity  $[Fe/H] \geq -1.3$ , the very metal poor stars (around  $[Fe/H] = -2.$ ) being a minor component (see Pap-I).

The SGR34 distribution has a defined strong metallicity limit at  $[Fe/H] = -0.7$  while the 30% of SGR12 stars have  $[Fe/H] \geq -0.7$ .

Fig. 7 shows for the first time that *the Sgr Pop A metallicity distribution presents significant structures*, certain metallicity ranges being more populated than others. In Sect. 6 we will show that this can be interpreted as a *variation of the Star Formation Rate (SFR) with time*.

## 6 THE AGE OF POP A

The first age estimate for the Sgr Pop A was made by MUSKKE, who fitted their decontaminated CMD of the SGR34 region with an isochrone of metallicity  $[Fe/H] =$

-1.2 and age 10 Gyr. They concluded that the bulk of the Sgr stars are significantly younger than typical Galactic globulars but older than intermediate age dSphs, as Carina. Subsequently, Mateo et al. (1996) studied a sample of Sgr stars projected in the same direction of the M55 globular cluster. They fitted the observed CMD (which is severely contaminated by M55 stars) with an isochrone of  $[Fe/H] = -0.5$  and age 12 Gyr.

Fahlman et al. (1996) also found evidences for the presence of Sgr stars in a field toward M55. The sparse Sgr MS in their CMD was equally well fitted by two different isochrones:  $[Fe/H] = -0.79$ ;  $age = 10Gyr$  or  $[Fe/H] = -1.27$ ;  $age = 14Gyr$ . Using the same set of isochrones they found an age of 16 Gyr for the Galactic globular clusters M55 and M4 and so confirmed a younger age for Sgr with respect to classical globulars.

While all the above determination of the age of Pop A rely on isochrone fitting (a technique often leading to ambiguous results and far from optimal in deriving age differences), MAL showed that the main CMD loci of Sgr are nearly coincident with those of the globular cluster Ter 7 ( $[Fe/H] \sim -1$  and  $\sim 4 - 6$  Gyr younger than typical Galactic globulars of similar metallicity<sup>§</sup>). This result provided (1) an empirical evidence of the younger age of Pop A with respect to standard old Galactic globulars and (2) the proof that the formation of globular clusters in Sgr ended with the star formation event that originated Pop A (see MoAL).

### 6.1 Distance and reddening -independent age estimates

MoAL presented the Age-Metallicity Relation (AMR) of the globular cluster system of the Sgr dSph, based on the measured  $\Delta V_{HB}^{TO}$  (the difference between the HB level and the magnitude of the TO point) and an  $age = f(\Delta V_{HB}^{TO}, [Fe/H])$  equation taken from Chaboyer, Demarque & Sarajedini (1996). They showed that, (1) the oldest clusters of the Sgr system (Ter 8 and M54) are coeval with the oldest Galactic globulars, (2) there is a significant range in age between the metal poor globulars of the Sgr dSph (i.e. Arp 2 is nearly 4 Gyr younger than Ter8 and M54) and (3) a significant chemical enrichment occurred in the time between the formation of Arp 2 ( $[Fe/H] = -1.84$ ) and the formation of Ter 7 ( $[Fe/H] \geq -1$ ), some 2-3 Gyr after.

For SGR34 we measured  $V(TO) = 21.5 \pm 0.1$  and  $V(HB) = 18.23 \pm 0.02$  (PAP-I),  $\Delta V_{HB}^{TO} = 3.27 \pm 0.1$  is derived, which places Sgr Pop A between Arp 2 and Ter 7 in the AMR of MoAL (see their Fig. 8), depending on the assumed metallicity. It is worth noting that the adopted  $V(HB)$  is the mean V magnitude of the red HB of Sgr, while the correct HB level should be the mean magnitude of the HB in the RR Lyrae region of the branch. This is expected to be fainter than  $V(RedHB)$  by  $\sim 0.05 - 0.15$  (see PAP-I), so the quoted  $\Delta V_{HB}^{TO}$  value can be regarded as an upper limit. Taking this correction into account the  $\Delta V_{HB}^{TO}$  of SGR34 is found to be virtually equal to that of Ter 7, confirming the result of MAL.

<sup>§</sup> The actual value of the metallicity of Ter 7 is subject of debate; see Fusi Pecci et al. 1995, Da Costa & Armandroff 1995 and Sarajedini & Layden 1997, for discussion.

The observables to estimate the relative ages of globular clusters are typically classified as *vertical* - when based on the *luminosity* of the TO points (as  $\Delta V_{HB}^{TO}$ ) - or *horizontal*, when based on the *color* of the TO (as  $\delta(B - V)$ ; see Stetson, Vandenberg & Bolte 1996 for discussion and references). Saviane, Rosenberg & Piotto (1997) recently presented a variant of the classical horizontal parameter for the (V;V-I) plane, i.e.  $\delta(V - I)_{2.2}$  the difference in color between the TO and the RGB at a level 2.2 mag brighter than the TO. The method is very promising<sup>¶</sup> since the preliminary results of Saviane, Rosenberg & Piotto (1997) suggest that  $\delta(V - I)_{2.2}$  is virtually independent of metallicity.

From our ridge line we obtain  $(V - I)_{TO} = 0.74 \pm 0.02$  and  $(V - I)_{2.2} = 1.07 \pm 0.02$  and finally  $\delta(V - I)_{2.2} = 0.33 \pm 0.03$ , the same as the well known young globular Pal 12. From Fig. 8 of Saviane, Rosenberg & Piotto (1997) and the calibration provided by the same authors we derived an age difference of  $\sim 4Gyr$  between Sgr and the bulk of the Galactic globulars, independently of the assumed metallicity.

### 6.2 Is Pop A a single-age population?

All the above age determinations are based on the following implicit hypothesis:

- (i) Pop A is a single-metallicity population or, at least, a meaningful *average metallicity* can be adopted.
- (ii) Pop A is a single-age population or, at least, a meaningful *average age* can be derived from the mean TO luminosity or color, once the metallicity is fixed.

Both of them are in large part false. Pop A cannot be treated as a single-metallicity population since there are clear observational evidences that there is a mixture of stars with significantly different abundances (Sect. 5). The derivation of an *average age* from the observed TO can be completely meaningless, since populations of different age and metallicity can have the TO placed at the same position.

Given the observed metallicity spread and TO morphology, two possible extreme scenarios may be invoked to describe the SFH of Sgr Pop A: (1) stars formed  $\sim 10$  Gyr ago in a short lapse of time ( $\leq 1Gyr$ ) from a very inhomogeneously enriched interstellar medium, with a wide range of abundances; (2) stars began to form at very early epoch and star formation continued for a quite long period ( $\geq 4Gyr$ ) from a chemically homogeneous interstellar medium (ISM) which was progressively enriched.

Option 1 seems contrary to the common wisdom on galaxy evolution, since it is expected that metallicity would increase with time. Furthermore it would be in contrast with the clear Age-Metallicity Relation defined by its globulars (MoAL).

<sup>¶</sup> However, as all the horizontal methods, it requires an exceptional accuracy in the determination of the observable, since differences of few hundredths of mag in  $\delta(V - I)_{2.2}$  can correspond to difference in age  $> 2$  Gyrs.

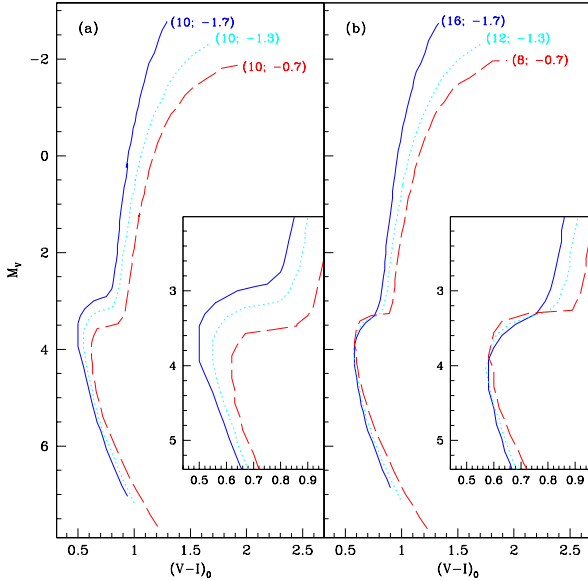


**Figure 8.** Theoretical expectations for the single-age case (panel a) and for the multi-age case (panel b). All isochrones are from the homogeneous set of Bertelli et al. (1994). Each isochrone is labeled according to the notation (age[Gyr]; [Fe/H]). The zoomed diagrams provide a closer view of the TO region.

### 6.2.1 Theoretical expectations

In Fig. 8 the two scenarios described above are illustrated according to the expectations of the stellar evolution theory. Here we adopt the homogeneous set of isochrones by Bertelli et al. (1994), but the results do not change if other isochrones are used<sup>||</sup>.

In panel (a) the *single-age + multi-metallicity* case is presented reporting three isochrones of *age* = 10 *Gyr* and with  $[Fe/H] = -1.7, -1.3, -0.7$ , respectively.

In panel (b) the *multi-age + multi-metallicity* case is presented reporting three isochrones of *age* = 16, 12, 8 *Gyr* and with  $[Fe/H] = -1.7, -1.3, -0.7$ , respectively. Younger isochrones has been associated with higher metal content.

The zoomed diagrams provide closer views of the TO region.

It is evident that, while the two groups of isochrones are very similar in their RGB characteristics, they significantly differ around the TO level.

The SGB and Upper MS of the in panel (a) are clearly detached one from another, with large color spread at the TO level ( $\Delta(V - I)_0 = 0.15$ ), while the isochrones reported in panel (b) are virtually superposed up to the base of the RGB. This is a well known effect (Sandage 1990 and references therein): at fixed age more metal rich populations have fainter TO points<sup>\*\*</sup>

In the SGR34 CMD, the observed color dispersion

<sup>||</sup> Very similar results have been obtained with the Cassisi et al. (1998) and the Vandenberg isochrones.

<sup>\*\*</sup> This is one of the aspects of the age/metallicity degeneracy,

around the ridge line of the stars with  $4.0 < M_V < 3.6$  and  $0.0 < V - I < 1.1$  is  $\sigma_{(V-I)} = 0.12$ , nearly equal to the photometric error at this level. Thus the data are perfectly consistent with nearly null intrinsic width and the extreme case *single age + multi metallicity* can be probably excluded. However such relatively high photometric errors at the TO level do not allow a clear-cut discrimination between any intermediate occurrence between the two extreme cases illustrated in Fig. 8.

### 6.2.2 Empirical age dating

In Fig. 9 the ridge line of SGR34 Pop A (open circles with central dot) is compared to the template ridge lines (continuous lines; dashed lines are adopted when the upper part of the line is implemented from a different source, see Sect. 5). The diameter of the open circles approximately corresponds to the extent of the uncertainty in the Sgr distance modulus ( $\sim \pm 0.3 \text{ dex}$ ). In the following, the comparison with the different templates will be performed discussing the various panels of Fig. 9.

- Panel (a), template: 47 Tuc. While this cluster provides a reasonable fit to the red edge of the RGB, the SGB and UMS sequences are clearly fainter and redder than those of SGR34. Note that the discrepancy cannot be recovered by different assumptions on the distance moduli and can be partially recovered only by assuming an error in  $E(V - I)$  of at least 0.1 *dex*, that is *very unlikely*. So, it can be safely concluded that *the Sgr stars at the same metallicity of 47 Tuc are significantly younger than this cluster*.

- Panel (b), template: Pal 1. This cluster has the same metallicity as 47 Tuc but is  $\sim 4 \text{ Gyr}$  younger, and provide a reasonable fit to the SGR34 faint sequences (it appears slightly “younger” but the two ridge lines are fully compatible within errors). *The Sgr stars at the same metallicity of 47 Tuc have an age similar to the globular cluster Pal 1, i.e.  $\sim 4 \text{ Gyr}$  younger than 47 Tuc.*

- Panel (c), template: M3. This template provides the best fit to the average RGB ridge line of SGR34, and indeed the metallicity distribution of Pop A peaks around the metallicity of M3. The fit to the SGB and UMS is not completely inconsistent but a younger template is probably needed. Unfortunately, a safe “younger” template at that metallicity is not available (at least in the V,I passbands). We tentatively conclude that *the stars of Sgr Pop A with metallicity around  $[Fe/H] = -1.3$  are probably younger than the M3 globular cluster (a classical old one)*. However the age difference between this component and M3 is probably smaller than the one between the metal rich component and 47 Tuc.

- Panel (d), template: M68. As shown in Sect. 5, the template provides a good fit to the blue edge of the Pop A RGB and the fit to the TO region is nearly perfect. We conclude that *the most metal poor stars of Sgr Pop A are as old as the oldest galactic globulars*. Note that also the most metal poor globulars belonging to the Sgr galaxy (M54 and Ter 8) are at least as old as M68 (MoAL, MAL, LS97).

an ubiquitous problem in the study of stellar populations (see Renzini & Fusi Pecci 1988, and references therein).

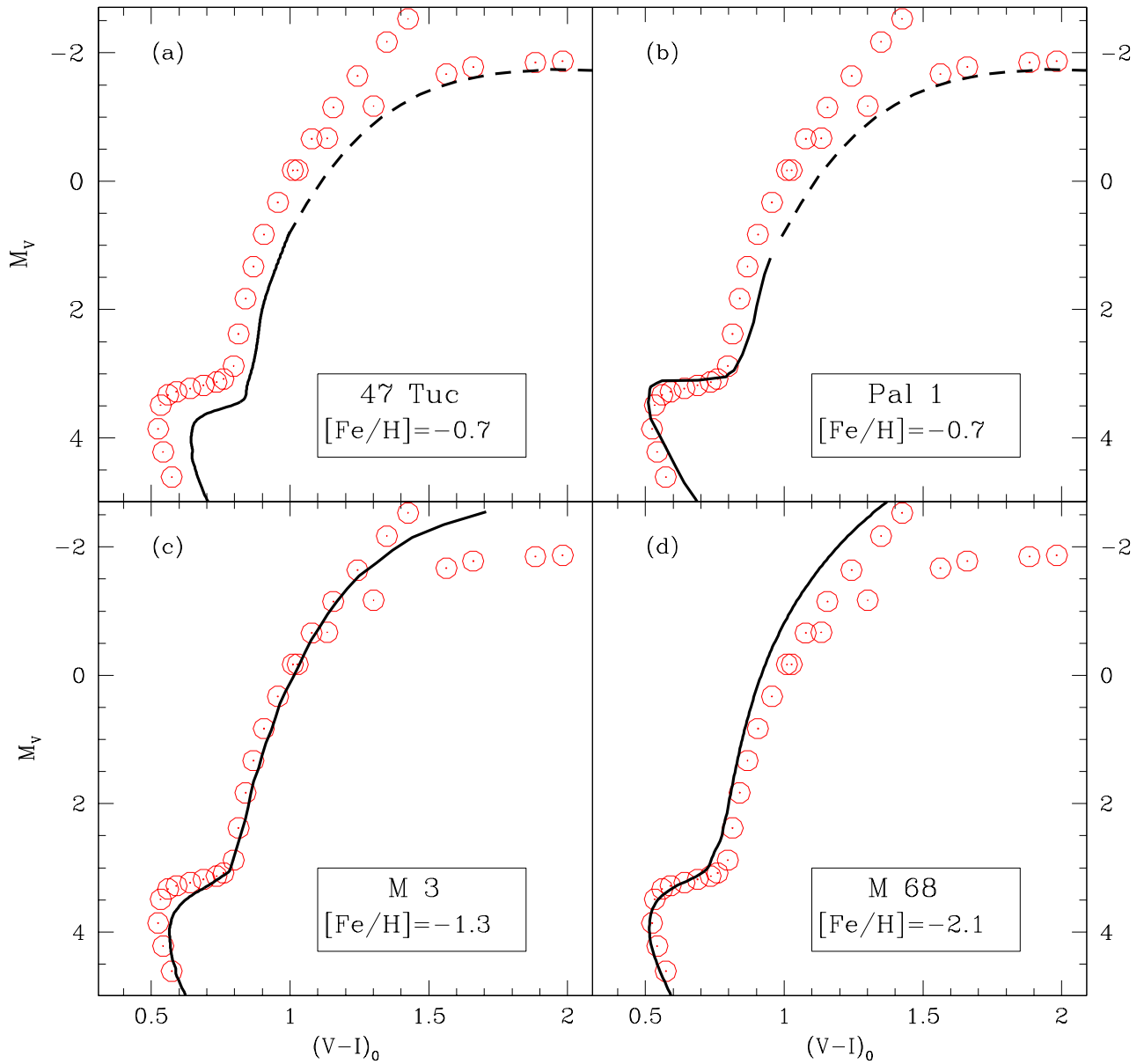


**Figure 9.** Comparisons between the SGR34 ridge line (open circles with central dot) and the ridge lines of the template clusters (continuous lines; the dashed line means that part of the ridge line has been complemented with data from a different source - see Sect. 5). All the lines have been reported to the absolute ( $M_V$ ;  $(V - I)_0$ ) plane with the assumptions described in Sect. 5. The radius of the open circles has approximately the dimension of the error box of the distance modulus of the Sgr galaxy. In the enclosed box in the lower left corner of each panel report the name and the metallicity of the template (panel (a): 47 Tuc; panel (b): Pal 1; panel (c): M 3; panel (d): M 68).

The above comparisons are clearly consistent with a scenario of chemical enrichment during a star formation phase lasted many billion years, in good agreement with the Globular Cluster AMR by MoAL. In the following sections we will couple these results with the metallicity distribution derived

in Sect. 5 to provide possible models of the Star Formation History of Pop A.

### 6.3 Setting the SF time scales

Though the SFR had a sharp decrease after the generation of stars at  $[Fe/H] = -0.7/-0.5$ , more recent low rate star formation could also take place in the Sgr galaxy (Pop B). Since this younger population is a minor component (see PAP-I) it is impossible to state if there was a temporal hiatus between the completion of Pop A and the onset of Pop B or if star formation continued at a lower rate. Furthermore, the empirical approach adopted for the analysis of Pop A cannot be applied to the Blue Plume stars, and we simply try to get an heuristic view by isochrone fitting. This would provide at least a zero-order global description of Pop A + Pop B as a whole, giving an idea of the SF time scales.

In Fig. 10 we have superimposed the isochrones of ( $[Fe/H] = -1.7$ ; age=16 Gyr), ( $[Fe/H] = -1.3$ ; age=12 Gyr) and ( $[Fe/H] = -0.7$ ; age=8 Gyr) from Bertelli et al. (1994) to the CMD of SGR34. To provide a reasonable fit to all the observed features we had to shift the isochrones by  $\Delta V = -0.1$  and  $\Delta(V - I) = -0.05$ .

Isocrones at  $[Fe/H] = -0.7$  of age 1 Gyr (long dashed line) and 4 Gyr (short dashed line) are also reported, and appear to bracket the whole Blue Plume. As we will see below the adoption of a higher metallicity for Pop B would shift the age estimates to younger ages.

According to Fig. 10, the main star formation period in the Sgr galaxy could have lasted for as much as  $\sim 8$  Gyr before some circumstance induced a sharp decrease in the star formation rate.

In Fig. 11 the CMD of the Blue Plume stars from the SGR34 and SGR12R samples is shown. This is the most populous CMD of such stars ever obtained. In the left panel isochrones at  $[Fe/H] = -0.7$  and ages of 0.5, 1, 2 and 4 Gyr (from left to right) are superimposed to the CMD. In the right panel isochrones of the same ages but with  $[Fe/H] = -0.4$  are reported.

From the inspection of Fig. 11 it can be concluded that the observed Blue Plume is consistent with a remarkably long lasting star formation event ( $\sim 3$  Gyr), or with many bursts separated by short lapses of quiescence. The time at which star formation definitively stopped depends on the actual metallicity of the stars, which is presently unknown. It is worth noting that if Pop B (or at least part of it) has solar or slightly super-solar metallicity, as could be argued from the preliminary results by Smecker-Hane et al. (1998; see also Da Costa 1999), an age as low as 60-100 million years cannot be excluded and the duration of the SF episode may shorten to  $< 0.5$  gyr.

### 6.4 Star Formation Histories

Following a suggestion of the Referee, we try to explore the possible Star Formation Histories of the Sgr Pop A applying the method described in detail by Rocha-Pinto & Maciel (1996, 1997). The method is aimed to the recovery of the stars birthrate as a function of time ( $B(t)$ ) from the presently observed metallicity distribution and the AMR of the considered stellar system, and it proved to be remarkably efficient in constraining the SFH of the Galactic Disc [see Rocha-Pinto & Maciel (1996) for assumptions, limitations and tests of the method].

Three basic elements are required:

(i) A metallicity distribution modeled with a Gaussian function. We fitted the metallicity distribution of the SGR34+SGR12 fields (taken as representative of the average Pop A, see Fig. 6) with a Gaussian with peak  $\langle [Fe/H] \rangle = -1.3$  and  $\sigma_{[Fe/H]} = 0.45$  dex.

(ii) An Age Metallicity Relation. Given the good agreement between the SF timescales derived in the previous sections and the GC AMR of MoAL we put together all these informations to constrain the global AMR. Three representative points were adopted from the above analysis of the Sgr field stars, i.e. ( $[Fe/H]; t_{[gyr]}$ ) =  $(-2.0; 0)$ ,  $(-1.3; 4)$ ,  $(-0.7; 8)$ , and four points from the fourth column of Table 5 by MoAL: Ter 8 =  $(-2.0; 0)$ , M54 =  $(-1.79; 1.5)$ , Arp 2 =  $(-1.84; 5)$  and Ter 7 =  $(-1.0; 8)$ . In the final time scale  $t = 0$  occurs 16 gyr ago and the age of Ter 7 and Arp 2 were increased by 0.5 gyr to impose exact coevity between Ter 7 and the more metal rich stars of Pop A, in agreement with the results by MAL. In the following analysis we will try different simple AMR models which can reasonably fit the distribution of these points in the  $t_{[gyr]}$  vs.  $[Fe/H]$  plane.

(iii) An assumed cosmic scatter in the abundance of the interstellar medium at any birthtime  $\sigma_z$ . Some indication on such scatter can be derived from the typical dispersion of data points in the  $t_{[gyr]}$  vs.  $[Fe/H]$  plane. We adopted two possible options:  $\sigma_z = 0.2$  dex and  $\sigma_z = 0.4$  dex.

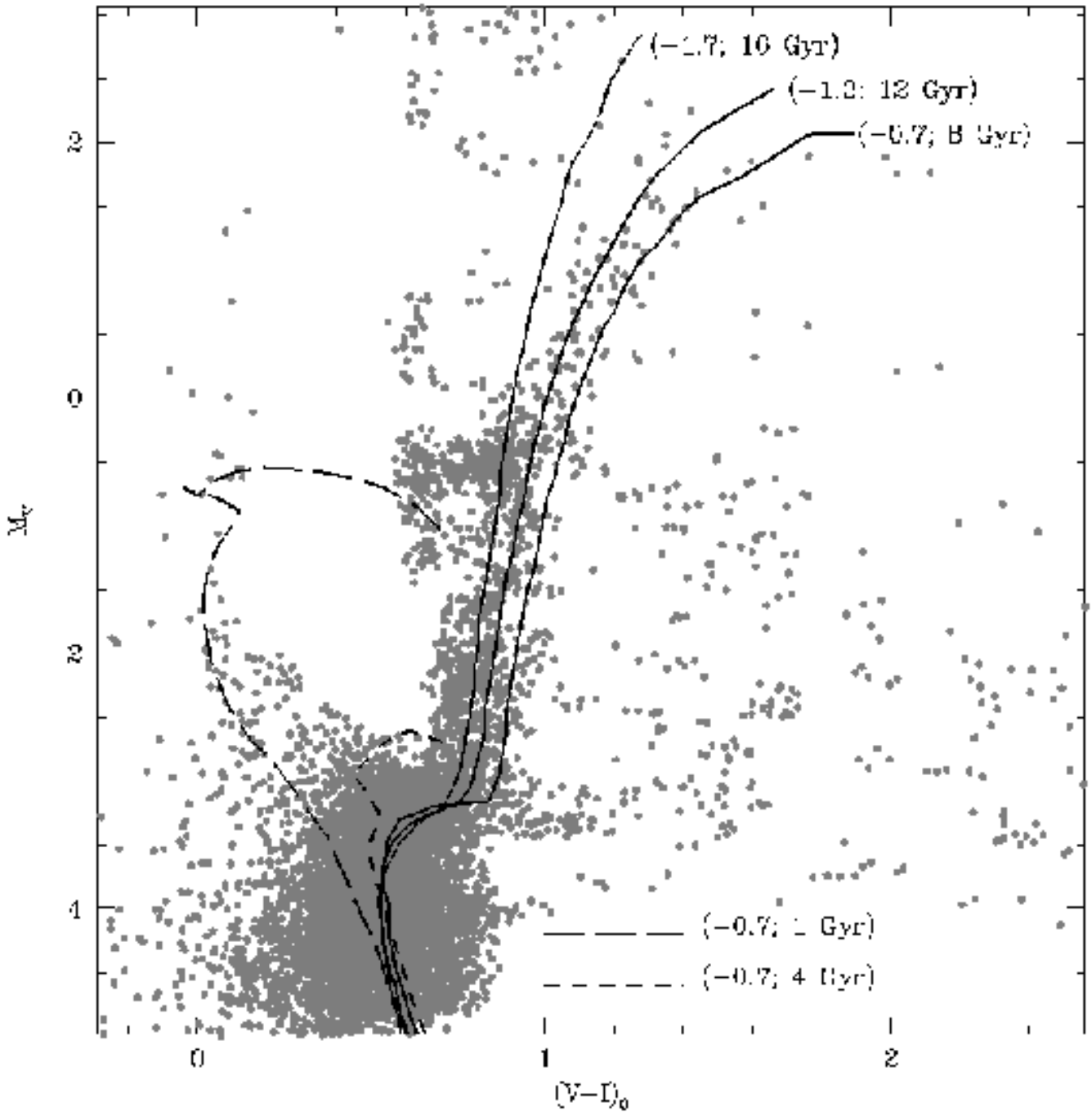
The time resolution of the derived  $B(t)$  is strongly limited by the coarseness and uncertainty of the metallicity distribution and of the AMR, and is estimated to be  $\geq 2$  gyr.

Fig. 12 reports the results of the experiments. In the left panels the adopted AMR models (continuous lines) are displayed, the GC points are represented by circles, the field points by squares. In the right panels the resulting  $B(t)$  (normalized to their peaks) are reproduced: each of them results from the coupling of the (unique) metallicity distribution with the assumed AMR. The continuous line represents the  $\sigma_z = 0.2$  dex option for the cosmic scatter, the dashed line represents the  $\sigma_z = 0.4$  dex one. In the upper  $x$ -axis the appropriate metallicity scale is schematically reported. It is important to recall that the latest time reported in the plots ( $t = 10$  gyr) is not the present time, which occurs 6 gyr later, in the adopted scale. The plot refers only to Pop A, whose star formation history ended  $\sim 6 - 8$  gyr ago.

We shortly discuss the results of Fig. 12, case by case:

Upper couple of panels: the simplest possible model of AMR has been adopted, a **linear** one. The resulting  $B(t)$  show a decline at early and late times, for both the  $\sigma_z$  options. The  $\sigma_z = 0.2$  case show a single broad peak at  $[Fe/H] \sim -1.3$ . The case with large cosmic scatter produce a double peaked  $B(t)$ , with  $\sim 5$  gyr between the two maxima. The linear model appears to be an obvious over-simplification of the enrichment history, resulting in a  $B(t)$  function too broad. One has to keep in mind that in the applied method the AMR states *how fast the clock runs at any given epoch*. The uniform run of the linear clock results in a period of intense star formation so extended to be incompatible with the observed time and metallicity scales.

Middle couple of panels: the AMR of the Sgr globulars is optimally fitted by an **exponential** model. The star formation rate is very low for the first  $\sim 6$  gyr, then a relatively short ( $\leq 2$  gyr) and intense period of star formation



**Figure 10.** Isochrones from the Bertelli et al. (1994) set superposed to the SGR34 CMD. The older isochrones (continuous lines) are labeled with the corresponding metallicity ( $[Fe/H]$ ) and age (Gyr). The isochrones bracketing the Blue Plume stars have metallicity  $[Fe/H] = -0.7$  and ages of 1 Gyr (long dashed line) and 4 Gyr (short dashed line), respectively.

occurred with rapid enrichment. This episode ceased rather abruptly and  $B(t) = 0$  before  $t = 9$  *gyr*. The two  $\sigma_z$  options give very similar results, both  $B(t)$  peaks at  $t \sim 8$  and  $[Fe/H] \sim -0.7$ . The  $\sigma_z = 0.4$  shows some sign of a second maximum at  $[Fe/H] \sim -1.5$ . We regard this scenario as the most likely, since the age and metallicity scale of the Sgr

globulars is much more robustly stated with respect to the field one.

Lower couple of panels: a **quadratic** AMR is adopted as a best fit model for the whole data set. Also in this case the star formation rate at early times is relatively low and the decrease of  $B(t)$  after  $t = 8$  *gyr* is rather abrupt. The

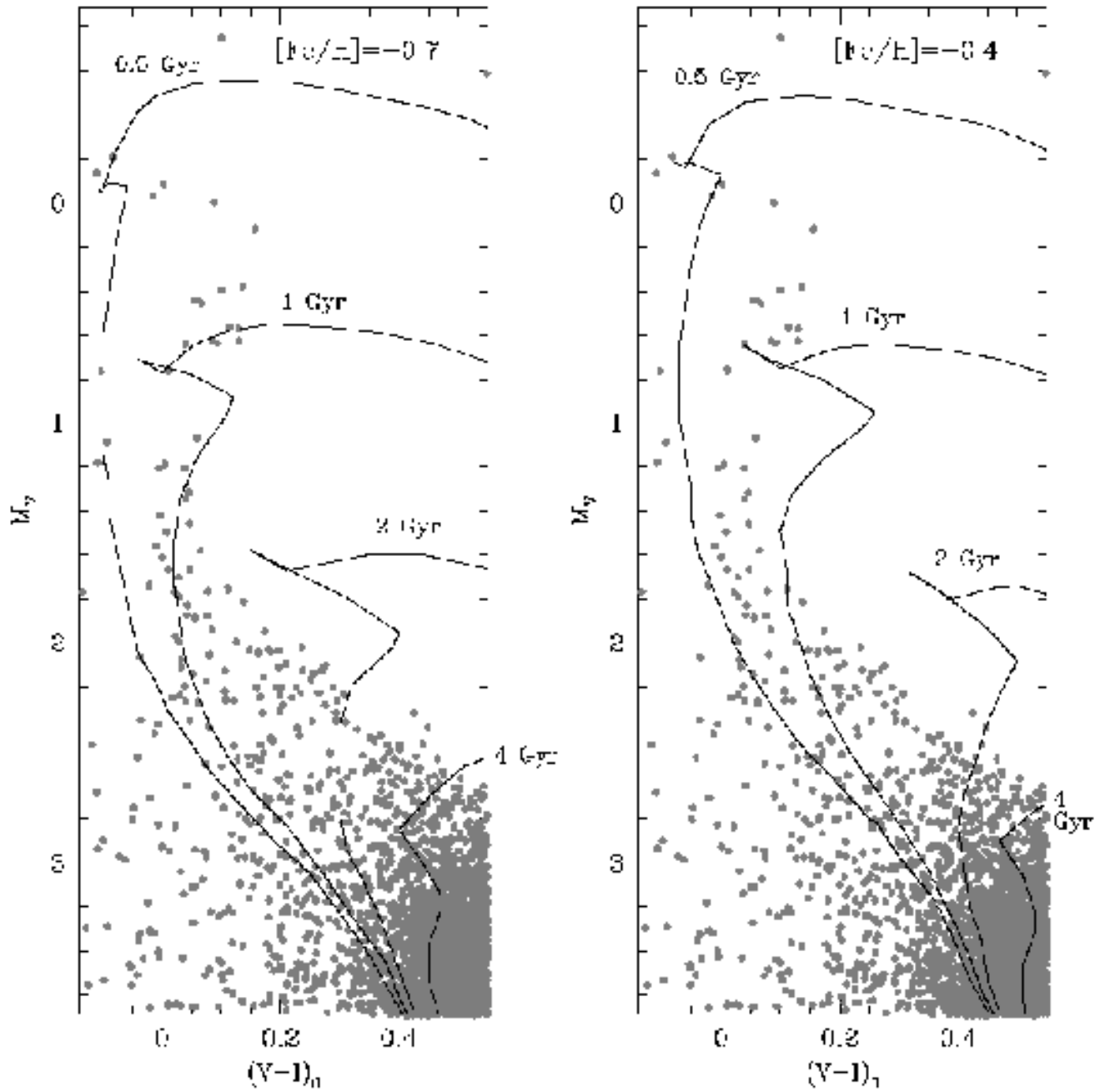


**Figure 11.** Isochrones from the Bertelli et al. (1994) set superposed to the SGR34+SGR12R CMD, centered on the Blue Plume stars. The isochrones are labeled with the corresponding age (Gyr) and have metallicity  $[Fe/H] = -0.7$  (left panel) and  $[Fe/H] = -0.4$  (right panel).

$\sigma_z = 0.4$  case shows again a secondary peak at  $[Fe/H] \sim -1.5$ .

There are some common characteristics of the derived SFHs which seem to be rather independent from the assumed AMR:

- $B(t)$  has a clear main peak, always occurring at  $6 \leq t \leq 8$  *gyr* and  $-1.3 \leq [Fe/H] \leq -0.7$ .
- In any case the SFR at early time is relatively low, and

in the two more realistic cases it rapidly falls after the main maximum.

- Any eventual secondary peak in the SFR is poorly constrained in time (from  $t \sim 3$  to  $t \sim 7$ , depending on the model) but it occurs at  $[Fe/H] \sim -1.5$ .

In the above scenario the Star Formation event that originated Pop A is presented as a continuous long lasting episode with a variable SFR, but the same general scheme is compatible with many different individual bursts. The only

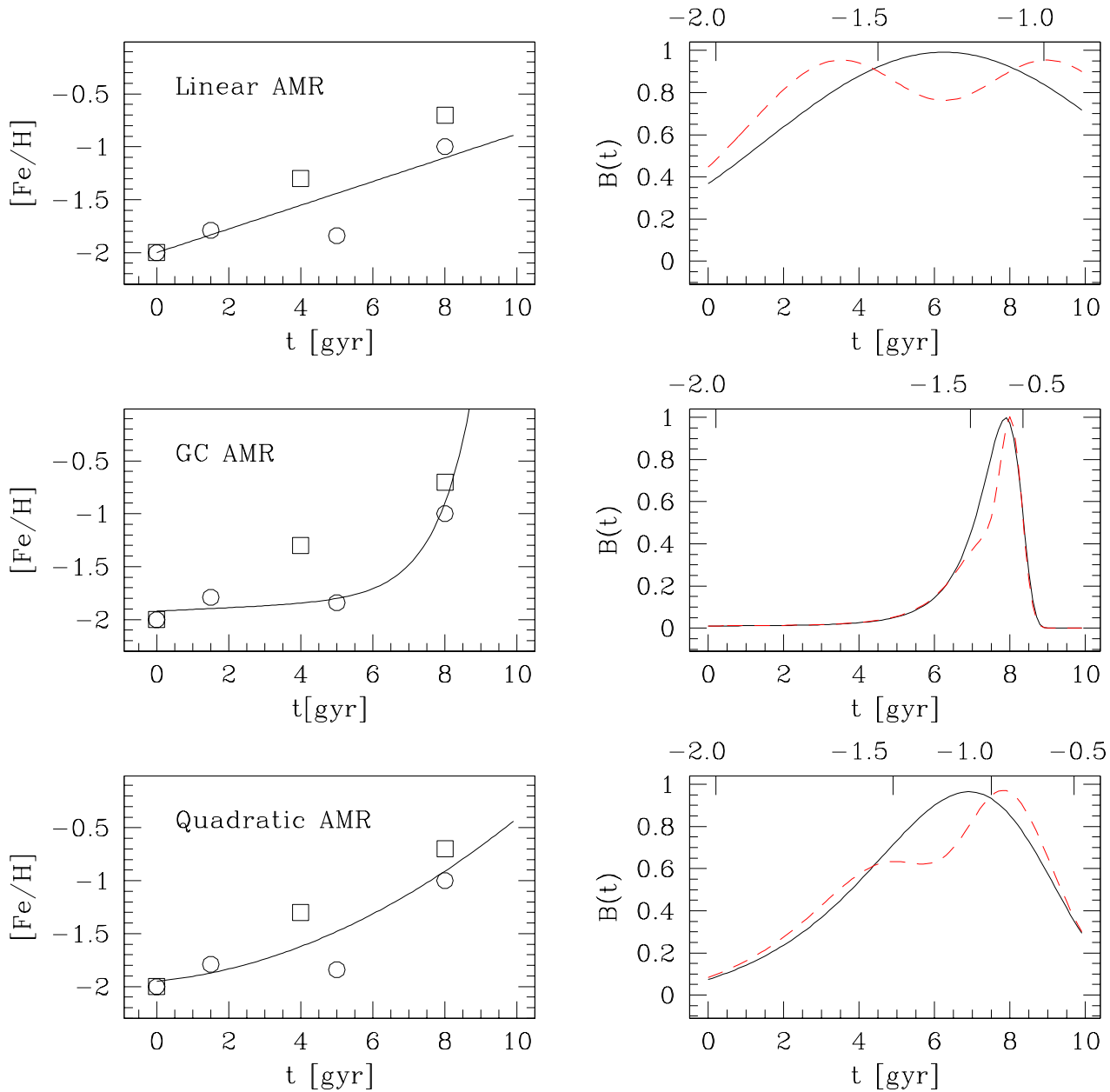


**Figure 12.** Possible Star Formation Histories for Pop A. In the left panels, the adopted AMR models are reported (continuous lines). Squares represent points derived from the present analysis, circles represent the Sgr globular clusters (from MoAL). The corresponding derived SFH are reported in the right panels. The continuous line represents the “low cosmic abundance scatter” case ( $\sigma_z = 0.2 dex$ ) and the dashed line the “high cosmic abundance scatter” one ( $\sigma_z = 0.4 dex$ ).

possibility of drawing a more detailed scheme is to couple accurate chemical pattern determinations (for instance  $[Fe/H]$  and  $\alpha$ -elements abundances) with deep photometry for a significant sample of Sgr Pop A stars.

## 7 SUMMARY AND CONCLUSIONS

The Color Magnitude Diagrams obtained from the SDGS have been statistically decontaminated and a detailed analysis of the cleaned diagrams have been performed, oriented to the search for constraints to the Star Formation History of the Sagittarius dwarf spheroidal galaxy.

The stellar content of the different regions sampled is

remarkably similar and it can be concluded that star formation in the Sgr dSph has been a very homogeneous process taking place under the same conditions on spatial scales of the order of the entire galaxy (see also Mateo, Olszewski & Morrison 1998).

The main population of the galaxy (Pop A) is composed by stars of metallicity ranging from  $[Fe/H] \sim -2.0$  to  $[Fe/H] \sim -0.7$ . A stellar component slightly more metal rich is present in the highest density clump of the galaxy (SGR12). A coarse metallicity distribution has been derived. About 60% of the Pop A stars have  $[Fe/H] \geq -1.3$ , the metal poor stars being a relatively minor component of the galaxy.

Based on the large color spread of the RGB (i.e., metallicity spread) and on the conversely narrow TO and SGB regions (consistent with a single TO point and SGB sequence, within the observational errors) a significant range in age has been deduced for Pop A stars, and related with the metallicity range.

The constraints on the AMR have been coupled with the metallicity distribution to derive the main characteristic of the Star Formation History. A remarkably robust general scheme emerges.

**Star Formation began in Sgr at low rate, at the epoch of formation of the oldest globular clusters of the Local Group** (see MoAL, Buonoanno et al. 1998, Stetson et al. 1998). **The ISM was progressively enriched and a main peak of the SFR occurred from 8 to 10 gyr ago when the mean metallicity was  $-1.3 \leq [Fe/H] \leq -0.7$ . During this main episode the globular cluster Ter 7 was also formed. Then the star formation ceased on timescales of order  $\leq 2$  gyr or less, depending on the adopted model. After this abrupt stop only minor star formation events took place (still on large spatial scales, see also PAP-I) up to 0.5 - 1 Gyr ago (or less) when the gas reservoir of the galaxy was completely exhausted** (see Koribalski, Johnston & Otrupceck 1995).

There are intrinsic difficulties in the study of this particular galaxy, mainly related to observational problems (Sect. 1) but also due to the peculiar SFH (Sect. 5 and 6). This is the reason why, despite of the huge efforts (SL95, MUSKKK, MAL, Mateo et al. 1996, FAL, IWGIS, LS97), only the *average properties* of the Sgr stellar populations have been derived until now.

Here we have pushed the analysis a significant step beyond, attempting for the very first time to provide a *differential* description of the stellar content of the Sgr dSph, *fitting all its observed properties simultaneously*. While still coarse and somehow qualitative, this scenario set the fundamental framework for the *second generation* studies of this stellar system, switching from a “monodimensional” average description to a “two-dimensional” view, from mean age and metallicity to Age-Metallicity relation and Star Formation History.

This is a key passage if we hope to take full advantage of the huge potentiality of the Sgr galaxy as a testbed for our models of dwarf galaxy formation and evolution and, above all, for our understanding of the links between star formation and galaxy-galaxy interactions.

## 7.1 Are Star Formation History and “orbital” history of Sgr coupled?

Based on radial velocity, a proper motion measurement and few reasonable assumptions, IWGIS found that the Sgr dSph lies in a very short period orbit ( $P = 0.76$  gyr) with a perigalactic point located at  $\sim 15$  kpc from the center of the Milky Way. The same authors argues that the orbit has remained the same for the whole lifetime of the galaxy. On these basis they suggest that Sgr managed to survive to so many close encounters with the Galaxy thanks to its high content of dark matter [see also Ibata & Lewis (1998)]. Even if a massive dark matter halo is actually embedding the Sgr stars and allowed the system to survive such unfavorable conditions, the damages of the tidal interactions are evident at the present time [see PAP-I and Mateo, Olszewski & Morrison (1998)] and the possibility that Sgr could be only an unbound remnant has been seriously considered [Helmi & White (1999)].

Now we know that the first stars formed in the Sgr galaxy nearly at the same time when first Galactic globulars formed. It is very difficult to conceive that  $\sim 15$  close passages to the center of the Milky Way and  $\sim 30$  Galactic disc crossings had no effect on the Star Formation and on the destiny of the ISM of the Sgr galaxy. On the other hand the stellar content and the SFH of Sgr appears quite “normal”, i.e. very similar to other dSphs which are supposed to evolve as unperturbed systems [as Draco or Sculptor, for instance; see Mateo (1998)]. In particular it is noteworthy that the formation of Pop A lasted  $\sim 8$  gyr with increasing SFR: this means that Sgr preserved (and self-enriched) most of its gas content for some 10 orbits. To “preserve its individuality”, this gas must have efficiently counteracted not only the tidal stress that ultimately stretched the whole galaxy, but also the ram pressure from the Galactic disc.

If Sgr evolved unperturbed in the orbit derived by IWGIS then many of our current believings about the connection between galaxy interactions and star formation probably should be revised [Schweizer (1998), Kennicutt (1998)].

Otherwise, some scenario should be envisaged in which the present orbit is only the final stage of a significant orbit evolution:

- Sgr passed most of its life in a wider orbit since some event [as for example a close encounter with the Magellanic Clouds, as suggested by Zhao (1998)] induced a significant orbital decay. One can concoct that the first close passage to the Galactic center coincided with the end of the star formation period that formed Pop A, or with the recent gasp which originated Pop B. The scenario proposed by Zhao (1998) could be consistent with the second hypothesis.
- Sgr originated from a gas cloud which is completing just now its process of collapse toward the potential well of the Galaxy. The collapse time is function of the distance from the “center of the collapse”. If at the “start” of the Galactic collapse the proto-Sgr found itself in the remote outskirts of the mass distribution that formed the Milky Way, it could have been left behind by the bulk of the proto-Galaxy that collapsed much more rapidly: in a free fall collapse regime [Eggen, Lynden Bell, Sandage (1962)] the collapse time at 40 kpc from the center is  $t_{ff} \sim 1$  gyr while at 150 kpc is  $t_{ff} \sim 10$  gyr. Sgr could have travelled for many gyr -

evolving as an unperturbed, isolated dSph - before reaching the inner regions of the Galaxy [see Blitz et al (1998), for a more general view of similar phenomena].

The first close encounter with the Milky Way could have lead to a strong tidal heating of Sgr, which bounded the galaxy on the present, low energy orbit. Also in this case, the onset of the SF episode associated with Pop B could have been triggered by this recent first interaction with the Galaxy.

## ACKNOWLEDGMENTS

We are indebted to an anonymous Referee for his contribution in improving the final version of the manuscript. We thank Flavio Fusi Pecci, Ken Mighell and, in particular, Monica Tosi for many useful discussions, Santi Cassisi and Don A. Vandenberg for providing their theoretical isochrones, Alfred Rosenberg for providing many templates and ridge lines in machine readable format. A very special thank is owed to Livia Origlia for a careful reading of a draft version of the manuscript.

Much of the data analysis has been made easier by the computer codes developed at the *Osservatorio Astronomico di Bologna* by Paolo Montegriffo. This research has made use of NASA's Astrophysics Data System Abstract Service.

This research has been partially funded by a Grant of the *Ministero delle Università e della Ricerca Scientifica e Tecnologica* (MURST) assigned to the project *Stellar Evolution* (national coordinator: Prof. V. Castellani).

## REFERENCES

Alcock, C. et al., 1997, ApJ, 474, 217  
Alard, C., 1996, ApJ, 458, L17  
Bellazzini, M., Ferraro, F.R., Buonanno, R., 1999, MNRAS, in press (PAP-I)  
Blitz L., Spergel D.N., Teuben P.J., Hartmann D., Burton W.B., 1998, ApJ, in press (astro-ph 9803251)  
Bruzual, G., Barbuy, B., Ortolani, S., Bica, E., Cuisinier, F., Lejeune, T., Schiavon, R.P., 1997, AJ, 114, 1531  
Buonanno, R., Corsi, C.E., Zinn, R., Fusi Pecci, F., Hardy, E., Suntzeff, N.B., 1998, ApJ, 501, L33  
Carretta E., Bragaglia A., 1998, A&A,  
Cassisi, S., Castellani, V., Degli Innocenti, S., Weiss, A., 1998, A&AS, 129, 267  
Da Costa G.S., 1998, in *Stellar Astrophysics for the Local Group*, A. Aparicio, A. Herrero and F. Sanchez eds., Cambridge: Cambridge University Press, p. 351  
Da Costa G.S., 1999, in *The Galactic Halo: Bright Stars & Dark Matter*, B.K. Gibson, T.S. Axelrod and M.E. Putnam eds., San Francisco, ASP, in press (astro-ph 9901258)  
Da Costa G.S., Armandroff T.E., 1990, AJ, 100, 162 (DCA90)  
Da Costa G.S., Armandroff T.E., 1995, AJ, 109, 2533  
Eggen O.J., Lynden-Bell D., Sandage A.R., 1962, ApJ, 136, 748  
Fahlman, G.G., Mandushev, G., Richer, H.B., Thompson, I.B., Sivaramakrishnan, A., 1996, ApJ, 459, L65 (FAL)  
Ferraro, F.R., Fusi Pecci, F., Bellazzini, M., 1995, A&A, 294, 80  
Ferraro, F.R., Carretta, E., Corsi, C.E., Fusi Pecci, F., Cacciari, C., Buonanno, R., Paltrinieri, B., Hamilton, D., 1997, A&A, 320, 757  
Helmi A., White S.D.M., 1999, MNRAS, in press (astro-ph 9901102)

Fusi Pecci, F., Bellazzini, M., Ferraro, F.R., Cacciari, C., 1995, AJ, 110, 1664  
Grebel, E., 1998, in *Dwarf Galaxies and Cosmology*, XVII Rencontre de Moriond, T.X. Thuan et al. Eds, Editions Frontieres, in press (astro-ph/9806191)  
Ibata R.A., Lewis G.F., 1998, ApJ, 500, 575  
Ibata, R.A., Gilmore, G., Irwin, M.J., 1994, Nature, 370, 194 (IGI-I)  
Ibata, R.A., Gilmore, G., Irwin, M.J., 1995, MNRAS, 277, 781 (IGI-II)  
Ibata, R.A., Wyse, R.F.G., Gilmore, G., Irwin, M.J., Suntzeff, N.B., 1997, AJ, 113, 634 (IWGIS)  
Johnston, K.V., 1998, ApJ, 495, 297  
Kaluzny, J., Wysocka, A., Stanek, K.Z., Krzemiński, W., 1998, Acta Astronomica, 48, 439  
Kennicutt R.C., 1998, in *Galaxies: Interactions and Induced Star Formation*, SAAS FEE vol. 26, Berlin, Springer  
Koribalski, B., Johnston, S., Otrupceck, R., 1995, MNRAS, 270, L43  
Layden, A. C., Sarajedini, A. 1997, ApJ, 486, L107 (LS97)  
Majevski, S.R., 1996, in *The Galactic Halo Inside ... and Out*, A. Sarajedini and H. Morrison Eds., ASP Conf. Ser., vol. 92, p. 119  
Marconi, G., Buonanno, R., Castellani, M., Iannicola, G., Pasquini, L., Molaro, P., A&A, 330, 453 (MAL)  
Mateo M., 1998, ARAA, 36, 435  
Mateo, M., Udalski, A., Szymanski, M., Kaluzny, J., Kubiak, M., Krzemiński, W., 1995a, AJ, 110, 1141 (MUSKKK)  
Mateo, M., Kubiak, M., Szymanski, M., Kaluzny, J., Krzemiński, W., Udalski, A., 1995b, AJ, 110, 1141 (MKSKKU)  
Mateo, M., Mirabal, N., Udalski, A., Szymanski, M., Kaluzny, J., Kubiak, M., Krzemiński, W., Stanek, K.Z., 1996, ApJ, 458, L13  
Mateo, M., Olszewski, E.W., Morrison, H., 1998, ApJ, 508, L55  
Mighell, K.J., Rich, R.M., Shara, M., Fall, S.M., 1996, AJ, 111, 2314 (MRSF)  
Mighell, K., Armandroff, T., Sarajedini, A., Layden, A., Mateo, M., Fusi Pecci, F., Ferraro, F., Buonanno, R., 1997, BAAS, 190, 35.05  
Montegriffo, P., Bellazzini, M., Ferraro, F.R., Martins, D., Sarajedini, A., Fusi Pecci, 1998, MNRAS, 294, 315 (MoAL)  
Nemec, J.M., Cohen, J.G., 1989, ApJ, 336, 780  
Olsen, K.A.G., Hodge, P.W., Mateo, M., Olszewski, E.W., Schommer, R.A., Suntzeff, N.B., Walker A.R., 1998, MNRAS, 300, 665  
Ortolani, S., Renzini, A., Gilmozzi, R., Marconi, G., Barbuy, B., Bica, E., Rich, S.M., 1995, Nature, 377, 701  
Pasquini, L. et al., 1999, in *The Stellar Content of the Local Group*, IAU Symp. 192, R. Cannon & P. Whitelock eds., S. Francisco: ASP, in press  
Rieke, G.H., Lebovski, M.J., 1985, ApJ, 288, 618 (RL)  
Rocha-Pinto H.J., Maciel W.J., 1996, MNRAS, 279, 447  
Rocha-Pinto H.J., Maciel W.J., 1997, MNRAS, 289, 882  
Rosenberg, A., Piotto, G., Saviane, I., Aparicio, A., Zaggia, S.R., 1998a, AJ, 115, 648  
Rosenberg, A., Piotto, G., Saviane, I., Aparicio, A., Gratton, R., 1998b, AJ, 115, 658  
Sarajedini, A., 1994, AJ, 107, 618  
Sarajedini, A., Norris, J.E., 1994, ApJS, 93,161  
Sarajedini, A., Layden, A., 1995, AJ, 109, 1086 (SL95)  
Sarajedini, A., Layden, A., 1997, AJ, 113, 264 (SL97)  
Saviane, I., Rosenberg, A., Piotto, G., 1997, in *Advances in Stellar Evolution*, R.T. Rood and A. Renzini eds., Cambridge: Cambridge University Press, p. 65  
Schweizer F., 1998, in *Galaxies: Interactions and Induced Star Formation*, SAAS FEE vol. 26, Berlin, Springer  
Smecker-Hane, T. A., Mc William, A., Ibata, R.A., 1998, BAAS, 192, 66.13

Stetson, P.B., Vandenberg, D.A., Bolte, M., 1996, *PASP*, 108, 560  
Whitelock, P.A., Irwin, M., Catchpole, R.M., 1996, *New Ast.*, 1,  
57 (WIC)  
Zhao, H., 1998, *ApJ*, 500, L149